HHS Public Access

Author manuscript

Brain Behav Immun. Author manuscript; available in PMC 2019 February 01.

Published in final edited form as:

Brain Behav Immun. 2018 February ; 68: 224–237. doi:10.1016/j.bbi.2017.10.021.

Selective activation of cannabinoid receptor-2 reduces neuroinflammation after traumatic brain injury via alternative macrophage polarization

Molly Braun[a], **Zenab T. Khan**[a,b], **Mohammad B. Khan**[c], **Manish Kumar**[d], **Ayobami Ward**[a], **Bhagelu R. Achyut**[f], **Ali S Arbab**[f], **David C. Hess**[c], **Md. Nasrul Hoda**[c,g], **Babak Baban**[c,e,h], **Krishnan M. Dhandapani**[a], and **Kumar Vaibhav**[a,g,*]

[a]Department of Neurosurgery, Medical College of Georgia, Augusta University

[b]Center for Nursing Research, Augusta University

[c]Department of Neurology, Medical College of Georgia, Augusta University

[d]European Molecular Biology Laboratory (EMBL), Monterontondo, Italy

[e]Department of Oral Biology, Dental College of Georgia, Augusta University

[f]Georgia Cancer Center, Augusta University

[g]Department of Medical Laboratory, Imaging, and Radiological Sciences, College of Allied Health Sciences, Augusta University

[h]Department of Surgery, Medical College of Georgia, Augusta University

Abstract

Inflammation is an important mediator of secondary neurological injury after traumatic brain injury (TBI). Endocannabinoids, endogenously produced arachidonate based lipids, have recently emerged as powerful anti-inflammatory compounds, yet the molecular and cellular mechanisms underlying these effects are poorly defined. Endocannabinoids are physiological ligands for two known cannabinoid receptors, CB1R and CB2R. In the present study, we hypothesized that selective activation of CB2R attenuates neuroinflammation and reduces neurovascular injury after TBI. Using a murine controlled cortical impact (CCI) model of TBI, we observed a dramatic upregulation of CB2R within infiltrating myeloid cells beginning at 72 hours. Administration of the selective CB2R agonist, GP1a (1–5 mg/kg), attenuated pro-inflammatory M1 macrophage polarization, increased anti-inflammatory M2 polarization, reduced edema development, enhanced

[*]*Address correspondence to*: Kumar Vaibhav, Ph.D., Department of Neurosurgery, Medical College of Georgia, Augusta, GA 30912, Ph: (706) 721-6331, Fax: (706) 721-7619, kvaibhav@augusta.edu.

Author Contributions

MB, ZTK, BB, KMD and KV conceptualized, designed, and performed experiments, analyzed data, and wrote the manuscript. MB, AW and MBK performed CBF analysis. ZTK and AW performed qPCR experiments. BB performed flow cytometric experiments. DH, MK and MNH assisted with experimental design and data interpretation. AS and BA acquired and assisted with the chimera preparation and analysis of MRI data.

cerebral blood flow, and improved neurobehavioral outcomes after TBI. In contrast, the CB2R antagonist, AM630, worsened outcomes. Taken together, our findings support the development of selective CB2R agonists as a therapeutic strategy to improve TBI outcomes while avoiding the psychoactive effects of CB1R activation.

Keywords

Cannabinoid receptor 2; Macrophage; Controlled cortical impact; Inflammation; Marijuana

1. Introduction

Traumatic brain injury (TBI) is a major cause of injury-related deaths and long-term disability. Cerebral edema, a life-threatening complication that presents in the hours and days after TBI, contributes to elevated intracranial pressure (ICP) (Catala-Temprano et al., 2007; Levin et al., 1991; Saul and Ducker, 1982), cerebral hypoperfusion (Catala-Temprano et al., 2007), inadequate tissue oxygenation (Narotam et al., 2009), brain herniation (Katayama et al., 1990; Lenzlinger et al., 2001; Sarabia et al., 1988), and a poor clinical patient prognosis (Eisenberg et al., 1990; Levin et al., 1991; Narayan et al., 2002). Neither neurosurgical nor medical approaches adequately reduce edema formation or improve cerebral perfusion (Bloch and Manley, 2007; Sahuquillo and Arikan, 2006). Given the high incidence rate of TBI, novel approaches are needed to ameliorate both the acute and long-term pathological outcomes following TBI.

The initial impact produces immediate mechanical damage and loss of tissue due to necrosis. This is followed by a coordinated set of immune responses that contribute towards both tissue repair and secondary neurological injury. Along these lines, we and others found a temporal and functional association between acute neuronal necrosis and the development of innate immune activation after both pre-clinical and clinical TBI (Braun et al., 2017; Czigner et al., 2007; Kawamata and Katayama, 2006; Laird et al., 2014). Macrophages are professional phagocytes that aid in clearance of cellular debris and tissue repair, yet the sustained release of pro-inflammatory mediators from infiltrating macrophages may exacerbate neuronal death, increase neurovascular injury, and contribute to long-term loss of white matter (Bartnik-Olson et al., 2014; Shi et al., 2015; Su and Bell, 2016). Although the molecular mechanisms underlying these opposing roles remain poorly defined, macrophages polarize along a continuum from a classical pro-inflammatory (M1) state to an alternative anti-inflammatory (M2) state. Notably, expression of both M1- and M2-like phenotypic markers are observed early after TBI, with the transient expression of M2 phenotypic markers yielding to a predominantly M1 phenotype that has been associated with the release of pro-inflammatory cytokines, edema development, the development of long-term adaptive immune responses, and neurodgeneration (Braun et al., 2017; Kim et al., 2016; Kumar et al., 2016). Thus, the development of therapeutic approaches to reduce pro-inflammatory M1 polarization may improve TBI outcomes.

Endocannabinoids, such as anandamide (N-arachidonoylethanolamide, AEA) and 2-arachidonoylglycerol (2-AG), are endogenously produced, arachidonate based lipids that

serve as physiological ligands for the cannabinoid receptors, CB1R and CB2R (Ashton and Moore, 2011; Buch, 2013; Munro et al., 1993). CB1R, which was originally detected in neurons, mediates the psychoactive effects of marijuana (Ashton and Moore, 2011; Buch, 2013; Ramirez et al., 2012). Conversely, CB2R is predominantly expressed on immune and endothelial cells and does not generate psychoactive activity (Anday and Mercier, 2005; Ramirez et al., 2012; Rom et al., 2013). Of note, inhibition of either CB1R or CB2R reversed the neuroprotective effects of minocycline (Lopez-Rodriguez et al., 2015) whereas inhibition of fatty acid amide hydrolase (FAAH), which boosts anandamide levels, increased anti-inflammatory microglia/macrophage activation and reduced neurodegeneration after TBI (Tchantchou et al., 2014). Thus, mechanistically defining the anti-inflammatory and neuroprotective roles of cannabinoid receptors may advance the therapeutic development to improve TBI outcomes.

In this study, we tested the hypothesis that administration of the selective CB2R agonist, GP1a [N-(piperidin-1-yl)-1-(2,4-dichlorophenyl)-1,4-dihydro-6-methylindeno[1,2-c]pyrazole-3-carboxamide], induces M2 macrophage polarization and improves TBI outcomes. We also explored whether administration of the selective CB2R antagonist, AM630 [6-Iodo-2-methyl-1-[2-(4-morpholinyl)ethyl]-1*H*-indol-3-yl](4-methoxyphenyl)methanone] would exacerbate neurovascular injury after TBI.

2. Materials and Methods

2.1. Controlled cortical impact

This study was conducted in accordance with the Guide for the Care and Use of Laboratory Animals (NIH Publication No. 85-23) and was approved by the Committee on Animal Use for Research and Education at Augusta University. C57BL/6 mice were used for bone marrow chimera and adoptive transfer studies, while CD1 mice were used for all other experiments. Briefly, male C57BL/6 mice or CD-1 mice (12–16 weeks old; Charles River Laboratories) were housed under a 12-h light/12-h dark cycle at 23 ± 1°C. Food and water were provided *ad libitum*. Mice were anesthetized with 2% isoflurane and subjected to either sham injury or controlled cortical impact, as detailed by our laboratory (Braun et al., 2017; Kimbler et al., 2012; Laird et al., 2010). Mice were placed in a stereotaxic frame and a circular craniotomy was made in the right parietal bone midway between the lambda and the bregma by carefully outlining a 2.0 mm radius bone flap centered at stereotaxic coordinates-AP= −2 mm from bregma; ML= +2.0 mm from mid line, leaving the dura intact. Mice were impacted at 3 m/s with 85 ms dwell time and 3 mm depression using a 3 mm diameter convex tip (PinPoint PCI3000 Precision Cortical Impactor, Hatteras Instruments, Cary, NC). Bone wax was used to seal the craniotomy, the incision was surgically stapled, and mice were placed in a clean warm cage until recovered. Sham-operated mice underwent the identical surgical procedures, but were not impacted. Body temperature was maintained at 37°C using a small animal temperature controller throughout all procedures (Kopf Instruments, Tujunga, CA, USA). For treatments, placebo (PBS), CB2R selective agonist GP1a (Tocris Bioscience, Bristol, UK) (1–5 mg/kg b.wt.) or the CB2R antagonist AM630 (Tocris Bioscience, Bristol, UK) (5 mg/kg b.wt.) were intraperitoneally administered at 10 min post-TBI.

2.2 Behavioral tests and Neurological scoring

2.2.1 Habituation—For all tasks, mice were habituated for thirty minutes in the behavior room prior to training/testing. All tasks were performed under identical lighting conditions at the same time each day. All behavioral chambers were cleaned with 70% ethanol cleaning solution before and after use.

2.2.2 Assessment of motor coordination—Motor coordination was assessed using an accelerating rotarod task. Mice were trained three days prior to injury and re-assessed at day 3 after TBI. Mice were placed on the rotarod moving at a constant speed of 4 rpm for thirty seconds followed by an acceleration to 30 rpm over the course of 4 minutes. The length of time each animal maintained balance while walking on top of the drum was recorded. Trials were ended when the animal either fell off the rod or clung to the rod for one complete rotation (Cernak et al., 2014). Motor coordination was further determined by measuring the time required to traverse a stationary 1 meter narrow beam (6 mm width) (Luong et al., 2011). Each mouse was tested three-times and the average was recorded. All behavioral analyses were done by investigators blinded to the experimental groups.

2.2.3 Open Field Test—Mice were placed in a 40 cm × 40 cm × 40 cm box for 10 minutes and activity was digitally recorded. Latency to enter the center zone and time spent in the center zone was recorded and analyzed using Ethovision XT video tracking software (Noldus Information Technology, Asheville, NC). Results were presented as mean ± SEM.

2.3 Tissue collection

At 72h post-TBI, mice were euthanized with 5% isoflurane. Blood was collected by cardiac puncture and placed into ice-cold heparinized tubes. Mice were next perfused transcardially with 30 mL of ice-cold phosphate buffered saline and brains were carefully removed. A 3-mm coronal brain section centered on the contusion was prepared using an acrylic brain matrix. Ipsilateral (injured) cerebral cortex from each brain was collected for different analyses, as detailed below. For histological and immunohistochemical analysis, brains were perfused with ice-cold phosphate buffered saline followed by 4% paraformaldehyde.

2.4 Immunostaining and Quantification

Five μm thick coronal sections were obtained from paraffin embedded tissue blocks and deparaffinized with xylene and alcohol gradients. Following an antigen retrieval step, deparaffinized sections were incubated with rabbit anti-CB2R antibody (1:200; Bioss#bs-2377R) overnight at 4°C followed by incubation with a fluorescently labeled secondary antibody (1:500; Jackson Laboratories, Burlingame, CA) for 1 hour. Tissue sections were mounted with Vectamount permanent mounting media (Vector Laboratories, CA). Fluorescent images were captured by Zeiss LSM 780 upright microscope integrated with Zen2.1 software and mean fluorescence intensity was calculated from five discrete area of ipsilateral cortex in each group using ImageJ software. The primary anti-CB2R antibody was commercially validated for staining. To further demonstrate the specificity of the primary and secondary antibodies in IHC, coronal sections were deparaffinized, retrieved for antigen and were blocked with 1xPBS containing 5% donkey serum for 30 min. After blocking, sections were incubated with either rabbit isotype control IgG (1:200; Bioss #

bs-0295P) or blocking buffer (no primary antibody) overnight. After incubation, sections were washed three times with 1xPBS containing 0.5% tween20 and incubated with secondary anti-rabbit IgG conjugated with Alexafluor594 (1:500; Jackson Laboratories, Burlingame, CA). After washing away unbound IgG, slides were mounted with anti-fade mounting media containing DAPI and were imaged for fluorescence by confocal microscopy (Carl Zeiss LSM 780). Images are shown as supplementary Fig 1 and 2.

2.5 Quantitative RT-PCR (qRT-PCR)

Total RNA was isolated using a SV RNA Isolation kit (Promega, Madison, WI) and reverse-transcribed into complementary deoxyribonucleic acid (cDNA) using iScript reagents on a programmable thermal cycler (C1000 Touch™ Thermal Cycler, Bio-Rad). 100 ng of cDNA was amplified in each real-time PCR using a BioRad iCycler and iTaq Universal SYBR Green reagents. Primers details are shown in Table 1. Product specificity was confirmed by melting curve analysis. Gene expression levels were quantified and data were normalized to 18S, a housekeeping gene that was unaffected by TBI (Laird et al., 2010). Data are expressed as mean fold change versus vehicle placebo treatment.

2.6 Preparative and analytical flow cytometry

Freshly isolated brain tissue was sieved through a cell strainer, followed by centrifugation (1,500 rpm, 5 min) to prepare single-cell suspensions. Blood was collected via cardiac puncture, as described above (section 2.3). Cells were incubated with antibodies against cell surface markers CD11b, CD68, CD206, CD45 and CB2R (All antibodies purchased from eBioSciences, San Diego, CA). Following a PBS wash, cells were fixed and permeabilized using a Fixation/Permeabilization Concentrate (Affymatrix eBioscience), and then incubated with antibodies for intracellular labeling of TNFα and IL-10 (BD BioSciences, Bedford, MA, USA). After a final wash, cells were analyzed using a 4-color flow cytometer (FACS Calibur, BD Biosciences, San Diego, CA, USA), and CellQuest software (BD Biosciences, San Jose, CA, USA), as described previously (Baban et al., 2005; Baban et al., 2013). Isotype-matched controls were analyzed to set the appropriate gates for each sample. For each marker, samples were analyzed in duplicate. To minimize false-positive events, the number of double-positive events detected with the isotype controls was subtracted from the number of double-positive cells stained with corresponding antibodies (not isotype control), respectively. Cells expressing a specific marker were reported as a percentage of the number of gated events.

2.7 Bone marrow chimera

C57BL/6 recipient mice were whole body irradiated with a sub-lethal dose of 6 Gy (Cs137). After 24h, recipient mice were intravenously injected with 5×10^6 bone marrow cells collected from transgenic mice expressing monomeric red fluorescent protein (RFP) (mCherry) under the direction of the human ubiqutin C promoter [B6(Cg)-Tyrc-2J Tg(UBC-mCherry)1Phbs/J; Jackson Laboratories, Stock#017614], as we detailed previously (Braun et al., 2017). Beginning at two weeks post-transplantation, 10 μL of blood was collected from the orbital sinus and RFP expression was measured in peripheral blood using flow cytometry. Blood from C57BL/6 mice without irradiation or RFP^+ cell transplantation were used as a control. We found efficient (>75%) engraftment of bone marrow by d28. On d30,

mice were subjected to sham/TBI and the presence of infiltrated RFP^+ myeloid cells were analyzed in brain tissue by flow cytometry.

2.8 Adoptive transfer of macrophages

Total bone marrow cells from naïve C57BL/6 mice were enriched and $CD11b^+$, $CD68^+$, $F4/80^+$ macrophages were consecutively sorted three times by magnetic bead isolation (Miltenyi Biotech) to achieve >95% purity. Purified macrophages were labeled with CFSE (Molecular Probes, Eugene, OR), a green fluorescent cell staining dye, as described previously (Sharma et al., 2010). A total of 6×10^5 cells/mouse were injected via the tail vein immediately after sham/TBI injury. To provide spatial analysis of macrophage trafficking into the brain, deeply anesthetized mice were perfused with PBS, followed by fixation with 4% paraformaldehyde in 0.1 M PBS (pH 7.4). Brains were post-fixed overnight in paraformaldehyde followed by cryoprotection with 30% sucrose (pH 7.4) until brains permeated. Serial coronal sections (12 μM) were prepared using a cryostat microtome and directly mounted onto glass slides. Anti-fade mounting media was added and glass cover slips were placed atop the slide. CFSE immunofluorescence was imaged using a LSM780 Meta confocal laser microscope and vendor supplied software (Carl Zeiss).

2.9 Magnetic resonance imaging (MRI)

MRI imaging was performed in the Augusta University Core Imaging Facility for Small Animals. Briefly, edema was quantified using high-resolution T2-weighed (T2W) images acquired using a horizontal Bruker 7.0T 20 cm bore BioSpec MRI spectrometer, as reported by our group (Kimbler et al., 2012; Laird et al., 2014). Each whole brain scan was made up of 16 slices. Anatomically matched sections were used for quantification and representative images were shown.

2.10 Laser speckle contrast imaging (LSCI)

LSCI was used to image cerebral perfusion and to record cerebral blood flow (CBF) before TBI (baseline) and after 24h post-TBI. Briefly, a midline incision was made to expose the skull. The skull then was cleaned with sterile phosphate-buffered saline (PBS) and non-toxic silicone oil was applied to improve imaging quality. Body temperature was maintained at 37 ± 0.5°C. Cerebral perfusion was calculated in regions of interest (ROIs) located between bregma and lambda in each hemisphere specifying the contusional and pericontusional cortex (ROI 2) vs contralateral cortex (ROI 1) using a Perimed PSI system with a 70 mW built-in laser diode for illumination and 1388 × 1038 pixels CCD camera installed 10 cm above the skull (speed 19 Hz, and exposure time 6 ms). Acquired high-resolution images were analyzed for changes in CBF (cerebral perfusion) using vendor supplied PIMSoft software and presented as mean perfusion values (Khan et al., 2015).

2.11 Statistical analysis

Multi-group comparisons were made using a one-way analysis of variance (ANOVA) followed by Newman-Keuls post-hoc test. Two group comparisons were analyzed by t-test. Results are expressed as mean ± SEM. A $p<0.05$ was considered to be statistically significant.

3. Results

3.1 Increased myeloid CB2R after TBI recruits and polarizes macrophages

qRT-PCR analysis revealed no significant differences in CB1R mRNA expression within the peri-contusional cortex, as compared to sham-operated mice (Fig 1A). In contrast, CB2R mRNA was increased ~15-fold ($p<0.001$; Fig 1B), suggesting a selective up-regulation of CB receptor subtypes after TBI. These data were supported by histological assessment, which showed widespread upregulation of $CB2R^+$ cells in traumatized brain ($p<0.001$; Fig 1C,D). To determine if $CB2R^+$ myeloid cells are responsible for these changes, we used an irradiation chimera approach whereby RFP-expressing bone marrow was transplanted into irradiated wild-type mice. Consistent with gene expression studies, a dramatic increase in the number of RFP^+CB2R^+ cells were observed in the peri-contusional cortex at 72h post-TBI ($p<0.001$; Fig 1E,F). Flow cytometric analysis determined that 52.7% of RFP^+ $CD11b^+$ $CD45^{HI}$ macrophages in the peri-contusional cortex expressed CB2R, whereas only 17.5% of cells were $CB2R^+$ in sham-operated brains ($p<0.001$; Fig 1E,F). Moreover, adoptive transfer of CFSE labeled macrophages (Fig 2A) identified the infiltration of $CB2R^+$ macrophages within the peri-contusional cortex after TBI, as assessed by immunohistochemistry ($p<0.001$; Fig 2B,C). In line with these findings, brain infiltration of peripheral macrophages ($CD45^{High}$) was minimized by administration of the CB2R agonist, GP1a (1 mg/kg, $p<0.05$; 3 mg/kg, $p<0.01$) after TBI (Fig 3). However, administration of the CB2R antagonist, AM630 treatment did not reflect any alteration in infiltrating macrophages population as compared to placebo treated TBI mice (Fig 3A, C). Interestingly, neither placebo nor agonist/antagonist treatment showed significant alterations in residential microglia ($CD45^{Low}$) [Fig 3B]. Sham mice with GP1a/AM630 treatment showed no significant changes in macrophages and microglia when compared to placebo treated sham (Supplementary Fig 3).

To functionally define the role of CB2R after TBI, mice were administered GP1a, a highly selective CB2R agonist, or AM630, a selective CB2R antagonist. GP1a dose-dependently attenuated M1 polarization and concomitantly increased M2 polarization after TBI ($p<0.001$; Fig 4A–D). In contrast, administration of AM630 had no effect on macrophage polarization, as compared to placebo-treated mice. In line with these observations, the post-traumatic mRNA expression of M1-associated cytokines, inducible nitric oxide synthase (iNOS), tumor necrosis factor-alpha (TNF-α), interleukin-1β (IL-1β) and interleukin-6 (IL-6) were suppressed by GP1a administration in contusional and pericontusional brain tissue (Fig 5). AM630 did not significantly affect expression levels of any of the M1-associated cytokines, as compared to placebo-treated mice (Fig 5). Conversely, GP1a significantly increased the expression of the M2-associated markers, arginase-1 (Arg-I) and interleukin-10 (IL-10), as compared to placebo-treated mice after TBI (Fig 5). In addition, GP1a, but not AM360, suppressed the induction of the leukocyte chemo-attractants, CCL2 and CXCL10, in the brain (Fig 5), suggesting a role for CB2R in the regulation of both macrophage recruitment and polarization after TBI.

3.2 CB2R activation reduces neurovascular injury after TBI

Post-treatment with GP1a (1–5 mg/kg) dose-dependently reduced cerebral edema, with a maximum effect noted with following administration of 3 mg/kg ($p<0.001$; Fig. 6A,B). In contrast, AM630 exhibited no effect on edema formation after TBI as compared to placebo-treated TBI. Edema development is frequently associated with reduced cerebral blood flow; thus, we next explored the effect of GP1a on cerebral perfusion using laser contrast speckle imaging. GP1a (1–5 mg/kg) significantly improved mean perfusion in the ipsilateral hemisphere at 24h post-TBI, as compared to placebo treated mice (Fig 7A,B). Similarly, 3 mg/kg GP1a maximally improved CBF, as compared to placebo treated mice after TBI ($p<0.001$). Administration of 5 mg/kg AM630 failed to improve cerebral perfusion, in line with the edema data. Sham mice with GP1a/AM630 treatment showed no changes in CBF as compared to placebo-treated sham (Supplementary Fig 4).

3.3 CB2R activation improves neurobehavioral outcomes after TBI

GP1a significantly improved motor coordination, as assessed by the stationary beam walk (Fig 8A) and rotarod test (Fig 8B) at 72h post-TBI. As was observed with edema and perfusion, administration of 3 mg/kg GP1a achieved maximal protection in the narrow beam test ($p<0.01$) and on the accelerated rotarod ($p<0.05$), as compared to placebo treated mice after TBI ($p<0.01$). As marijuana is anecdotally used as an anxiolytic, we also examined the anxiety level of mice after TBI. Placebo treated mice showed higher latency ($p<0.01$) to first entry into center zone and spent less time in center zone ($p<0.001$) as compared to sham (Fig 9A–C), suggestive of anxious behavior. Administration of GP1a reduced the latency to enter into center zone, as compared to placebo treated mice ($p<0.01$) whereas AM630 administration had no effect on latency (not significantly different from placebo, $p<0.05$ vs. GP1a treated mice) [Fig. 9B]. Mice treated with 3 mg/kg GP1a also spent significantly more time in center zone, as compared with placebo ($p<0.001$) and AM630 ($p<0.01$) treated mice, indicative of reduced anxiety after TBI ($p<0.01$) [Fig. 9C]. Neither GP1a nor AM630 influenced motor coordination or anxious behavior when administered to sham-operated mice, as compared to placebo treated sham (Supplementary Fig 5–6).

4. Discussion

In this report, we demonstrated that CB2R was prominently expressed on infiltrating macrophages within the peri-contusional cortex and activation of CB2R with GP1a, the most specific CB2R ligand currently available, increased anti-inflammatory, M2 macrophage polarization. We further showed that CB2R activation reduced edema volume, improved cerebral perfusion, and enhanced neurological outcomes after TBI. Thus, selective targeting of CB2R may be an efficacious therapeutic target to promote long-term outcomes after neurotrauma.

Anecdotal evidence and early stage clinical investigations suggest a medicinal role for phytocannabinoids, such as marijuana (*Cannabis sativa*), in the treatment of glaucoma, cachexia, nausea, emesis, and neuropathic pain (Croxford and Yamamura, 2005; Di Marzo and Petrocellis, 2006; Zhang and Ho, 2015); however, the potential for recreational abuse and addiction may ultimately limit the clinical utility of marijuana (Allen et al., 2016).

Marijuana is comprised of equimolar amounts of Δ^9-tetrahydrocannabinol (Δ^9-THC), the principal psychoactive constituent a classical partial agonist at CB1R/CB2R, and cannabidiol (CBD), a nonpsychoactive cannabinoid that accounts for 40% of the Cannabis plant extract (Campos et al., 2012; Pertwee, 2008; Syed et al., 2014), suggesting a potential interplay between two cannabinoid receptors CB1R and CB2R. Interestingly, CBD is neuroprotective after cerebral hypoxia-ischemia in immature pigs, at least in part, via activation of CB2R (Castillo et al., 2010; Pazos et al., 2013); however, CBD reduced human BBB permeability changes and produced anti-depressant and anxiolytic effect independently from CB2R (de Mello Schier et al., 2014; Hind et al., 2016). Thus, the development of specific CB2R agonists, which lack activity at CB1R, may enhance neurological outcomes after brain injury without the associated psychoactive side effects.

Repeated administration of O-1966, a selective CB2R agonist, attenuated blood-brain barrier disruption and limited neuronal degeneration during the acute phase after TBI (de Mello Schier et al., 2014). In addition, O-1966, reduced edema, attenuated macrophage/microglial activation, and was associated with recovery of acute motor and exploratory deficits (Elliott et al., 2011). Another CB2R agonist JWH-133 expedited post-stroke recovery by driving neuroblast cells to the injured site, suggesting a possible role for CB2R in neurogenesis and functional recovery (Bravo-Ferrer et al., 2017). However, the selectivity for CB2R in mediating these effects remains unclear. For example, O-1966 reduced cocaine-induced conditioned place preference; however, these effects were maintained in global CB2R knockout mice, suggesting O-1966 may exhibit off-target effects from CB2R (Ignatowska-Jankowska et al., 2013)). Coupled with pharmacological studies showing lower selectivity (~200 fold) of O-1966 (K_i for CB2R 20.9 – 25.1 nM; for CB1R 4071–6039 nM) and JWH133 (Ki for CB2R 3.4 nM; Ki for CB1R 677 nM) for CB2R over CB1R (Steffens and Pacher, 2012), attention have moved toward the development of more selective CB2R agonists. As described previously, inhibition of CB1 receptor activation is protective during cerebral ischemia/reperfusion injury while inhibition of CB2R receptor activation is detrimental (Zhang et al., 2008) therefore, the greatest degree of neuroprotection may be obtained by treatment with a CB2R agonist having low affinity for CB1R activation. In this report, we have utilized GP1a, which exhibits ~1000 fold higher preference for CB2R over CB1R (Ki values are 0.037 and 363 nM for CB2R and CB1R, respectively.

CB2R is widely and highly expressed in a range of leukocytes and appears to be the key mediator of cannabinoid regulation of inflammation and immune functions (Ashton and Glass, 2007). For example, blockade of the CB2R receptor with SR145528 inhibits splenocyte proliferation and induces apoptosis in vitro (McKallip et al., 2002a; McKallip et al., 2002b). CB2R also regulates B and T cell differentiation, and the balance of proinflammatory T helper (T_H1) to anti-inflammatory T_H2 cytokines (Ziring et al., 2006). CB2R activation also suppresses neutrophil migration and differentiation (Nilsson et al., 2006), but induces natural killer cell migration (Kishimoto et al., 2005). In macrophages, CB2R stimulation suppresses proliferation and the release of pro-inflammatory factors such as NO, IL-12p40, and TNF-α, inhibits phagocytosis, and reduces IL-2 signaling to T-cells (Chuchawankul et al., 2004). Taken together, these studies on CB2R receptors in leukocytes are consistent with an anti-inflammatory and immuno-suppressive role. This has been supported in recent years by demonstrations that CB2R regulates inflammation in a diverse

range of animal models, including but not limited to gastro-intestinal inflammation (Massa and Monory, 2006), acute hind paw inflammation (Conti et al., 2002), pulmonary inflammation (Berdyshev et al., 1998), and inflammation-induced hyperalgesia (Valenzano et al., 2005).

TBI is associated with prolonged inflammation due to both central and peripheral immune responses (Gyoneva and Ransohoff, 2015; Karve et al., 2016). Along these lines, we and others observed a transient increase in peripheral macrophage infiltration as early as 24 hours post-injury, peaking at day three, and persisting for several weeks post-TBI (Braun et al., 2017; Hsieh et al., 2013; Jin et al., 2012; Kumar et al., 2016). On the other hand, microglia, the resident macrophages within the CNS, showed a biphasic increase at day seven and again at one month post-TBI (Hsieh et al., 2013). In the present study, we observed a significant increase in infiltrating $CB2R^+$ macrophages whereas $CB2R^+$ were not altered significantly at day 3 post-TBI. Importantly, administration of GP1a selectively reduced macrophage infiltration with no discernable effect on microglia at day 3 post-injury. As the selective effect of Gp1a may be time dependent, we cannot completely exclude a role for CB2R in the regulation of microglial activation and/or polarization. Nonetheless, our data support a critical role for CB2R activation on peripheral macrophage activation/polarization during the acute phase after TBI.

Our observation of increased myeloid CB2R expression, with no changes in CB1R expression after TBI, is in line with increased CB2R binding, with no change in CB1R density, after fluid-percussion injury in newborn piglets (Donat et al., 2014). Functionally, GP1a increased M2 macrophage polarization, reduced the expression of pro-inflamamtory mediators (TNFα, IL1β, IL6, CCl2, CXCL10 and iNOS) and enhanced the expression of anti-inflammatory mediators (IL10 and ArgI) in contusional and pericontusional brain tissue after TBI, supporting the notion that the proposed neuroprotective actions of CB2R agonists are mediated by reducing inflammation after TBI. Although the precise mechanisms whereby CB2R regulates macrophage polarization and neurological protection remains largely undefined, toll-like receptor 4 (TLR4) is an important mediator of inflammation after brain injury (Braun et al., 2017; Laird et al., 2014; Zhang et al., 2014). We reported that early activation of myeloid TLR4 increased M1 macrophage polarization (Braun et al., 2017) and enhanced edema formation after experimental TBI (Laird et al., 2014). In the present study, GP1a reduced M1 macrophage activation, decreased the expression of pro-inflamamtory cytokine/chemokines, and attenuated edema formation after TBI. These observations raise the interesting and unexplored possibility that CB2R may limit myeloid TLR4 signaling as a mechanism to reduce neuroinflammatory activation after TBI. Indeed, pharmacological activation of CB2R inhibited toll-like receptor expression, including TLR4 expression after spinal cord injury (Adhikary et al., 2011). In agreement, CB2R activation attenuated D-galactosamine/lipopolysaccharide (LPS)–induced acute liver failure by inducing an M1 to M2 shift in macrophages and by regulating the expression of miR-145, which negatively regulates TLR4 signaling (Tomar et al., 2015). Furthermore, we recently reported that myeloid TLR4 activation mediated the chronic activation of T_H1/T_H17 polarization after experimental TBI (Braun et al., 2017). Although unexplored in this report, cannabinoids decrease T_H17 polarization in a murine model of multiple sclerosis (Kozela et al., 2013). Thus, modulation of myeloid CB2R may influence both short- and long-term

recovery after TBI, at least in part, via regulation of TLR4 signaling pathways, a possibility that is the subject of active investigation by our laboratory.

Robust neuro-inflammatory reactions are associated with both acute neurovascular changes and chronic behavioral deficits (Hou et al., 2017; Peterson et al., 2015; Pottker et al., 2017). Regional and global CBF changes lead to asymmetric hemispheric neural activity patterns and contribute toward the development of long-term anxiety, cognitive, balance, and motor deficits after TBI (Hou et al., 2017; Plomgaard et al., 2017; Salehi et al., 2017). Our result in congruence with previous study showing impaired sports-related function in American Football players after TBI. These players after brain injury showed strong evidence of late-life depression and short-term physical dysfunctions (Vos et al., 2017). Further, preclinical study with TBI rats showed immediate cognitive and motor deficits after injury (Chen et al., 2016). Interestingly, GP1a treated mice showed protected motor ability on stationary narrow beam and accelerating rotarod. In addition, elevated post-traumatic anxiety was alleviated by GP1a treatment. On contrary, CB2R antagonist AM630-treated mice showed elevated anxiety and enhance thigomotaxis after TBI. Our findings are in line with a report showing mice administered β-caryophyllene, a CB2R agonist, exhibited anxiolytic and anti-depressant phenotype, effects that were reversed by co-administration of the CB2 receptor antagonist AM630 (Bahi et al., 2014). Taken together, our preclinical data suggest that targeted activation of CB2R may provide a novel therapeutic target to improve motor and psychiatric function after TBI.

Conclusions

Inflammatory activation may produce both detrimental and reparative functions after TBI, suggesting a delicate balance is required to improve long-term outcomes. In this study, we show that GP1a, the most selective CB2R agonist developed to date, improves neurological outcomes, improves motor functions and reduces anxiety after experimental TBI. These effects were associated with increased anti-inflammatory M2 polarization, suggesting a critical role of CB2R in peripheral immune cells in recovery from TBI. Our findings support the further development of highly selective CB2R agonists as a potential theraeptic approach to exploit the beneficial of endocannabinoids without the associated psychoactive side effects of CB1R activation.

Supplementary Material

Refer to Web version on PubMed Central for supplementary material.

Acknowledgments

Financial support for this project was provided by a grant from the Augusta University Research Institute and by grants from the National Institutes of Health (R03HD094606, R01NS065172, R21NS075774 and R03NS084228).

References

Adhikary S, Li H, Heller J, Skarica M, Zhang M, Ganea D, Tuma RF. Modulation of inflammatory responses by a cannabinoid-2-selective agonist after spinal cord injury. J Neurotrauma. 2011; 28:2417–27. [PubMed: 21970496]

Allen S, Stewart SH, Cusimano M, Asbridge M. Examining the Relationship Between Traumatic Brain Injury and Substance Use Outcomes in the Canadian Population. Subst Use Misuse. 2016; 51:1577–1586. [PubMed: 27484302]

Anday JK, Mercier RW. Gene ancestry of the cannabinoid receptor family. Pharmacol Res. 2005; 52:463–6. [PubMed: 16118055]

Ashton CH, Moore PB. Endocannabinoid system dysfunction in mood and related disorders. Acta Psychiatr Scand. 2011; 124:250–61. [PubMed: 21916860]

Ashton JC, Glass M. The cannabinoid CB2 receptor as a target for inflammation-dependent neurodegeneration. Curr Neuropharmacol. 2007; 5:73–80. [PubMed: 18615177]

Baban B, Hansen AM, Chandler PR, Manlapat A, Bingaman A, Kahler DJ, Munn DH, Mellor AL. A minor population of splenic dendritic cells expressing CD19 mediates IDO-dependent T cell suppression via type I IFN signaling following B7 ligation. Int Immunol. 2005; 17:909–19. [PubMed: 15967784]

Baban B, Liu JY, Abdelsayed R, Mozaffari MS. Reciprocal relation between GADD153 and Del-1 in regulation of salivary gland inflammation in Sjogren syndrome. Exp Mol Pathol. 2013; 95:288–97. [PubMed: 24060278]

Bahi A, Al Mansouri S, Al Memari E, Al Ameri M, Nurulain SM, Ojha S. beta-Caryophyllene, a CB2 receptor agonist produces multiple behavioral changes relevant to anxiety and depression in mice. Physiol Behav. 2014; 135:119–24. [PubMed: 24930711]

Bartnik-Olson BL, Holshouser B, Wang H, Grube M, Tong K, Wong V, Ashwal S. Impaired neurovascular unit function contributes to persistent symptoms after concussion: a pilot study. J Neurotrauma. 2014; 31:1497–506. [PubMed: 24735414]

Berdyshev E, Boichot E, Corbel M, Germain N, Lagente V. Effects of cannabinoid receptor ligands on LPS-induced pulmonary inflammation in mice. Life Sci. 1998; 63:Pl125–9. [PubMed: 9718090]

Bloch O, Manley GT. The role of aquaporin-4 in cerebral water transport and edema. Neurosurg Focus. 2007; 22:E3.

Braun M, Vaibhav K, Saad N, Fatima S, Brann DW, Vender JR, Wang LP, Hoda MN, Baban B, Dhandapani KM. Activation of Myeloid TLR4 Mediates T Lymphocyte Polarization after Traumatic Brain Injury. J Immunol. 2017; 198:3615–3626. [PubMed: 28341672]

Bravo-Ferrer I, Cuartero MI, Zarruk JG, Pradillo JM, Hurtado O, Romera VG, Diaz-Alonso J, Garcia-Segura JM, Guzman M, Lizasoain I, Galve-Roperh I, Moro MA. Cannabinoid Type-2 Receptor Drives Neurogenesis and Improves Functional Outcome After Stroke. Stroke. 2017; 48:204–212. [PubMed: 27899748]

Buch SJ. Cannabinoid receptor 2 activation: a means to prevent monocyte-endothelium engagement. Am J Pathol. 2013; 183:1375–7. [PubMed: 24055258]

Campos AC, Moreira FA, Gomes FV, Del Bel EA, Guimaraes FS. Multiple mechanisms involved in the large-spectrum therapeutic potential of cannabidiol in psychiatric disorders. Philos Trans R Soc Lond B Biol Sci. 2012; 367:3364–78. [PubMed: 23108553]

Castillo A, Tolon MR, Fernandez-Ruiz J, Romero J, Martinez-Orgado J. The neuroprotective effect of cannabidiol in an in vitro model of newborn hypoxic-ischemic brain damage in mice is mediated by CB(2) and adenosine receptors. Neurobiol Dis. 2010; 37:434–40. [PubMed: 19900555]

Catala-Temprano A, Claret Teruel G, Cambra Lasaosa FJ, Pons Odena M, Noguera Julian A, Palomeque Rico A. Intracranial pressure and cerebral perfusion pressure as risk factors in children with traumatic brain injuries. J Neurosurg. 2007; 106:463–6.

Cernak I, Wing ID, Davidsson J, Plantman S. A novel mouse model of penetrating brain injury. Front Neurol. 2014; 5:209. [PubMed: 25374559]

Chen H, Chan YL, Nguyen LT, Mao Y, de Rosa A, Beh IT, Chee C, Oliver B, Herok G, Saad S, Gorrie C. Moderate traumatic brain injury is linked to acute behaviour deficits and long term mitochondrial alterations. Clin Exp Pharmacol Physiol. 2016; 43:1107–1114. [PubMed: 27557565]

Chuchawankul S, Shima M, Buckley NE, Hartmann CB, McCoy KL. Role of cannabinoid receptors in inhibiting macrophage costimulatory activity. Int Immunopharmacol. 2004; 4:265–78. [PubMed: 14996418]

Conti S, Costa B, Colleoni M, Parolaro D, Giagnoni G. Antiinflammatory action of endocannabinoid palmitoylethanolamide and the synthetic cannabinoid nabilone in a model of acute inflammation in the rat. Br J Pharmacol. 2002; 135:181–7. [PubMed: 11786493]

Croxford JL, Yamamura T. Cannabinoids and the immune system: potential for the treatment of inflammatory diseases? J Neuroimmunol. 2005; 166:3–18. [PubMed: 16023222]

Czigner A, Mihaly A, Farkas O, Buki A, Krisztin-Peva B, Dobo E, Barzo P. Kinetics of the cellular immune response following closed head injury. Acta Neurochir (Wien). 2007; 149:281–9. [PubMed: 17288002]

de Mello Schier AR, de Oliveira Ribeiro NP, Coutinho DS, Machado S, Arias-Carrion O, Crippa JA, Zuardi AW, Nardi AE, Silva AC. Antidepressant-like and anxiolytic-like effects of cannabidiol: a chemical compound of Cannabis sativa. CNS Neurol Disord Drug Targets. 2014; 13:953–60. [PubMed: 24923339]

Di Marzo V, Petrocellis LD. Plant, synthetic, and endogenous cannabinoids in medicine. Annu Rev Med. 2006; 57:553–74. [PubMed: 16409166]

Donat CK, Fischer F, Walter B, Deuther-Conrad W, Brodhun M, Bauer R, Brust P. Early increase of cannabinoid receptor density after experimental traumatic brain injury in the newborn piglet. Acta Neurobiol Exp (Wars). 2014; 74:197–210. [PubMed: 24993629]

Eisenberg HM, Gary HE Jr, Aldrich EF, Saydjari C, Turner B, Foulkes MA, Jane JA, Marmarou A, Marshall LF, Young HF. Initial CT findings in 753 patients with severe head injury. A report from the NIH Traumatic Coma Data Bank. J Neurosurg. 1990; 73:688–98. [PubMed: 2213158]

Elliott MB, Tuma RF, Amenta PS, Barbe MF, Jallo JI. Acute effects of a selective cannabinoid-2 receptor agonist on neuroinflammation in a model of traumatic brain injury. J Neurotrauma. 2011; 28:973–81. [PubMed: 21332427]

Gyoneva S, Ransohoff RM. Inflammatory reaction after traumatic brain injury: therapeutic potential of targeting cell-cell communication by chemokines. Trends Pharmacol Sci. 2015; 36:471–80. [PubMed: 25979813]

Hind WH, England TJ, O'Sullivan SE. Cannabidiol protects an in vitro model of the blood-brain barrier from oxygen-glucose deprivation via PPARgamma and 5-HT1A receptors. Br J Pharmacol. 2016; 173:815–25. [PubMed: 26497782]

Hou J, Nelson R, Wilkie Z, Mustafa G, Tsuda S, Thompson FJ, Bose P. Mild and Mild-to-Moderate Traumatic Brain Injury-Induced Significant Progressive and Enduring Multiple Comorbidities. J Neurotrauma. 2017; 34:2456–2466. [PubMed: 28376701]

Hsieh CL, Kim CC, Ryba BE, Niemi EC, Bando JK, Locksley RM, Liu J, Nakamura MC, Seaman WE. Traumatic brain injury induces macrophage subsets in the brain. Eur J Immunol. 2013; 43:2010–22. [PubMed: 23630120]

Ignatowska-Jankowska BM, Muldoon PP, Lichtman AH, Damaj MI. The cannabinoid CB2 receptor is necessary for nicotine-conditioned place preference, but not other behavioral effects of nicotine in mice. Psychopharmacology (Berl). 2013; 229:591–601. [PubMed: 23652588]

Jin X, Ishii H, Bai Z, Itokazu T, Yamashita T. Temporal changes in cell marker expression and cellular infiltration in a controlled cortical impact model in adult male C57BL/6 mice. PLoS One. 2012; 7:e41892. [PubMed: 22911864]

Karve IP, Taylor JM, Crack PJ. The contribution of astrocytes and microglia to traumatic brain injury. Br J Pharmacol. 2016; 173:692–702. [PubMed: 25752446]

Katayama Y, Tsubokawa T, Miyazaki S, Kawamata T, Yoshino A. Oedema fluid formation within contused brain tissue as a cause of medically uncontrollable elevation of intracranial pressure: the role of surgical therapy. Acta Neurochir Suppl (Wien). 1990; 51:308–10. [PubMed: 2089924]

Kawamata T, Katayama Y. Surgical management of early massive edema caused by cerebral contusion in head trauma patients. Acta Neurochir Suppl. 2006; 96:3–6.

Khan MB, Hoda MN, Vaibhav K, Giri S, Wang P, Waller JL, Ergul A, Dhandapani KM, Fagan SC, Hess DC. Remote ischemic postconditioning: harnessing endogenous protection in a murine model of vascular cognitive impairment. Transl Stroke Res. 2015; 6:69–77. [PubMed: 25351177]

Kim CC, Nakamura MC, Hsieh CL. Brain trauma elicits non-canonical macrophage activation states. J Neuroinflammation. 2016; 13:117. [PubMed: 27220367]

Kimbler DE, Shields J, Yanasak N, Vender JR, Dhandapani KM. Activation of P2X7 promotes cerebral edema and neurological injury after traumatic brain injury in mice. PLoS One. 2012; 7:e41229. [PubMed: 22815977]

Kishimoto S, Muramatsu M, Gokoh M, Oka S, Waku K, Sugiura T. Endogenous cannabinoid receptor ligand induces the migration of human natural killer cells. J Biochem. 2005; 137:217–23. [PubMed: 15749836]

Kozela E, Juknat A, Kaushansky N, Rimmerman N, Ben-Nun A, Vogel Z. Cannabinoids decrease the th17 inflammatory autoimmune phenotype. J Neuroimmune Pharmacol. 2013; 8:1265–76. [PubMed: 23892791]

Kumar A, Alvarez-Croda DM, Stoica BA, Faden AI, Loane DJ. Microglial/Macrophage Polarization Dynamics following Traumatic Brain Injury. J Neurotrauma. 2016; 33:1732–1750. [PubMed: 26486881]

Laird MD, Sukumari-Ramesh S, Swift AE, Meiler SE, Vender JR, Dhandapani KM. Curcumin attenuates cerebral edema following traumatic brain injury in mice: a possible role for aquaporin-4? J Neurochem. 2010; 113:637–48. [PubMed: 20132469]

Laird MD, Shields JS, Sukumari-Ramesh S, Kimbler DE, Fessler RD, Shakir B, Youssef P, Yanasak N, Vender JR, Dhandapani KM. High mobility group box protein-1 promotes cerebral edema after traumatic brain injury via activation of toll-like receptor 4. Glia. 2014; 62:26–38. [PubMed: 24166800]

Lenzlinger PM, Morganti-Kossmann MC, Laurer HL, McIntosh TK. The duality of the inflammatory response to traumatic brain injury. Mol Neurobiol. 2001; 24:169–81. [PubMed: 11831551]

Levin HS, Eisenberg HM, Gary HE, Marmarou A, Foulkes MA, Jane JA, Marshall LF, Portman SM. Intracranial hypertension in relation to memory functioning during the first year after severe head injury. Neurosurgery. 1991; 28:196–9. discussion 200. [PubMed: 1997886]

Lopez-Rodriguez AB, Siopi E, Finn DP, Marchand-Leroux C, Garcia-Segura LM, Jafarian-Tehrani M, Viveros MP. CB1 and CB2 cannabinoid receptor antagonists prevent minocycline-induced neuroprotection following traumatic brain injury in mice. Cereb Cortex. 2015; 25:35–45. [PubMed: 23960212]

Luong TN, Carlisle HJ, Southwell A, Patterson PH. Assessment of motor balance and coordination in mice using the balance beam. J Vis Exp. 2011

Massa F, Monory K. Endocannabinoids and the gastrointestinal tract. J Endocrinol Invest. 2006; 29:47–57. [PubMed: 16751708]

McKallip RJ, Lombard C, Fisher M, Martin BR, Ryu S, Grant S, Nagarkatti PS, Nagarkatti M. Targeting CB2 cannabinoid receptors as a novel therapy to treat malignant lymphoblastic disease. Blood. 2002a; 100:627–34. [PubMed: 12091357]

McKallip RJ, Lombard C, Martin BR, Nagarkatti M, Nagarkatti PS. Delta(9)-tetrahydrocannabinol-induced apoptosis in the thymus and spleen as a mechanism of immunosuppression in vitro and in vivo. J Pharmacol Exp Ther. 2002b; 302:451–65. [PubMed: 12130702]

Munro S, Thomas KL, Abu-Shaar M. Molecular characterization of a peripheral receptor for cannabinoids. Nature. 1993; 365:61–5. [PubMed: 7689702]

Narayan RK, Michel ME, Ansell B, Baethmann A, Biegon A, Bracken MB, Bullock MR, Choi SC, Clifton GL, Contant CF, Coplin WM, Dietrich WD, Ghajar J, Grady SM, Grossman RG, Hall ED, Heetderks W, Hovda DA, Jallo J, Katz RL, Knoller N, Kochanek PM, Maas AI, Majde J, Marion DW, Marmarou A, Marshall LF, McIntosh TK, Miller E, Mohberg N, Muizelaar JP, Pitts LH, Quinn P, Riesenfeld G, Robertson CS, Strauss KI, Teasdale G, Temkin N, Tuma R, Wade C, Walker MD, Weinrich M, Whyte J, Wilberger J, Young AB, Yurkewicz L. Clinical trials in head injury. J Neurotrauma. 2002; 19:503–57. [PubMed: 12042091]

Narotam PK, Morrison JF, Nathoo N. Brain tissue oxygen monitoring in traumatic brain injury and major trauma: outcome analysis of a brain tissue oxygen-directed therapy. J Neurosurg. 2009; 111:672–82. [PubMed: 19463048]

Nilsson O, Fowler CJ, Jacobsson SO. The cannabinoid agonist WIN 55,212-2 inhibits TNF-alpha-induced neutrophil transmigration across ECV304 cells. Eur J Pharmacol. 2006; 547:165–73. [PubMed: 16928371]

Pazos MR, Mohammed N, Lafuente H, Santos M, Martinez-Pinilla E, Moreno E, Valdizan E, Romero J, Pazos A, Franco R, Hillard CJ, Alvarez FJ, Martinez-Orgado J. Mechanisms of cannabidiol neuroprotection in hypoxic-ischemic newborn pigs: role of 5HT(1A) and CB2 receptors. Neuropharmacology. 2013; 71:282–91. [PubMed: 23587650]

Pertwee RG. The diverse CB1 and CB2 receptor pharmacology of three plant cannabinoids: delta9-tetrahydrocannabinol, cannabidiol and delta9-tetrahydrocannabivarin. Br J Pharmacol. 2008; 153:199–215. [PubMed: 17828291]

Peterson TC, Maass WR, Anderson JR, Anderson GD, Hoane MR. A behavioral and histological comparison of fluid percussion injury and controlled cortical impact injury to the rat sensorimotor cortex. Behav Brain Res. 2015; 294:254–63. [PubMed: 26275924]

Plomgaard AM, Alderliesten T, Austin T, van Bel F, Benders M, Claris O, Dempsey E, Fumagalli M, Gluud C, Hagmann C, Hyttel-Sorensen S, Lemmers P, van Oeveren W, Pellicer A, Petersen TH, Pichler G, Winkel P, Greisen G. Early biomarkers of brain injury and cerebral hypo- and hyperoxia in the SafeBoosC II trial. PLoS One. 2017; 12:e0173440. [PubMed: 28328980]

Pottker B, Stober F, Hummel R, Angenstein F, Radyushkin K, Goldschmidt J, Schafer MKE. Traumatic brain injury causes long-term behavioral changes related to region-specific increases of cerebral blood flow. Brain Struct Funct. 2017

Ramirez SH, Hasko J, Skuba A, Fan S, Dykstra H, McCormick R, Reichenbach N, Krizbai I, Mahadevan A, Zhang M, Tuma R, Son YJ, Persidsky Y. Activation of cannabinoid receptor 2 attenuates leukocyte-endothelial cell interactions and blood-brain barrier dysfunction under inflammatory conditions. J Neurosci. 2012; 32:4004–16. [PubMed: 22442067]

Rom S, Zuluaga-Ramirez V, Dykstra H, Reichenbach NL, Pacher P, Persidsky Y. Selective activation of cannabinoid receptor 2 in leukocytes suppresses their engagement of the brain endothelium and protects the blood-brain barrier. Am J Pathol. 2013; 183:1548–58. [PubMed: 24055259]

Sahuquillo J, Arikan F. Decompressive craniectomy for the treatment of refractory high intracranial pressure in traumatic brain injury. Cochrane Database Syst Rev. 2006 Cd003983.

Salehi A, Zhang JH, Obenaus A. Response of the cerebral vasculature following traumatic brain injury. J Cereb Blood Flow Metab. 2017 271678x17701460.

Sarabia R, Lobato RD, Rivas JJ, Cordobes F, Rubio J, Cabrera A, Gomez P, Munoz MJ, Madera A. Cerebral hemisphere swelling in severe head injury patients. Acta Neurochir Suppl (Wien). 1988; 42:40–6. [PubMed: 3189019]

Saul TG, Ducker TB. Effect of intracranial pressure monitoring and aggressive treatment on mortality in severe head injury. J Neurosurg. 1982; 56:498–503. [PubMed: 6801218]

Sharma MD, Hou DY, Baban B, Koni PA, He Y, Chandler PR, Blazar BR, Mellor AL, Munn DH. Reprogrammed foxp3(+) regulatory T cells provide essential help to support cross-presentation and CD8(+) T cell priming in naive mice. Immunity. 2010; 33:942–54. [PubMed: 21145762]

Shi H, Hu X, Leak RK, Shi Y, An C, Suenaga J, Chen J, Gao Y. Demyelination as a rational therapeutic target for ischemic or traumatic brain injury. Exp Neurol. 2015; 272:17–25. [PubMed: 25819104]

Steffens S, Pacher P. Targeting cannabinoid receptor CB(2) in cardiovascular disorders: promises and controversies. Br J Pharmacol. 2012; 167:313–23. [PubMed: 22612332]

Su, E., Bell, M. Frontiers in Neuroscience Diffuse Axonal Injury. In: Laskowitz, D., Grant, G., editors. Translational Research in Traumatic Brain Injury. CRC Press/Taylor and Francis Group (c) 2016 by Taylor & Francis Group, LLC; Boca Raton (FL): 2016.

Syed YY, McKeage K, Scott LJ. Delta-9-tetrahydrocannabinol/cannabidiol (Sativex(R)): a review of its use in patients with moderate to severe spasticity due to multiple sclerosis. Drugs. 2014; 74:563–78. [PubMed: 24671907]

Tchantchou F, Tucker LB, Fu AH, Bluett RJ, McCabe JT, Patel S, Zhang Y. The fatty acid amide hydrolase inhibitor PF-3845 promotes neuronal survival, attenuates inflammation and improves functional recovery in mice with traumatic brain injury. Neuropharmacology. 2014; 85:427–39. [PubMed: 24937045]

Tomar S, Zumbrun EE, Nagarkatti M, Nagarkatti PS. Protective role of cannabinoid receptor 2 activation in galactosamine/lipopolysaccharide-induced acute liver failure through regulation of

macrophage polarization and microRNAs. J Pharmacol Exp Ther. 2015; 353:369–79. [PubMed: 25749929]

Valenzano KJ, Tafesse L, Lee G, Harrison JE, Boulet JM, Gottshall SL, Mark L, Pearson MS, Miller W, Shan S, Rabadi L, Rotshteyn Y, Chaffer SM, Turchin PI, Elsemore DA, Toth M, Koetzner L, Whiteside GT. Pharmacological and pharmacokinetic characterization of the cannabinoid receptor 2 agonist, GW405833, utilizing rodent models of acute and chronic pain, anxiety, ataxia and catalepsy. Neuropharmacology. 2005; 48:658–72. [PubMed: 15814101]

Vos BC, Nieuwenhuijsen K, Sluiter JK. Consequences of Traumatic Brain Injury in Professional American Football Players: A Systematic Review of the Literature. Clin J Sport Med. 2017

Zhang D, Li H, Li T, Zhou M, Hao S, Yan H, Yu Z, Li W, Li K, Hang C. TLR4 inhibitor resatorvid provides neuroprotection in experimental traumatic brain injury: implication in the treatment of human brain injury. Neurochem Int. 2014; 75:11–8. [PubMed: 24858944]

Zhang M, Martin BR, Adler MW, Razdan RK, Ganea D, Tuma RF. Modulation of the balance between cannabinoid CB(1) and CB(2) receptor activation during cerebral ischemic/reperfusion injury. Neuroscience. 2008; 152:753–60. [PubMed: 18304750]

Zhang MW, Ho RC. The Cannabis Dilemma: A Review of Its Associated Risks and Clinical Efficacy. J Addict. 2015; 2015:707596. [PubMed: 26539302]

Ziring D, Wei B, Velazquez P, Schrage M, Buckley NE, Braun J. Formation of B and T cell subsets require the cannabinoid receptor CB2. Immunogenetics. 2006; 58:714–25. [PubMed: 16924491]

Highlights

- Inflammation is an important mediator of secondary neurological injury after TBI
- Activation of CB2R attenuates inflammation and reduces neurovascular injury after TBI
- CB2R agonist, GP1a polarized macrophages into anti-inflammatory (M2) phenotypes
- GP1a reduced edema, enhanced cerebral blood flow, and improved behavioral outcomes
- CB2R antagonist, AM630 worsened physiological and behavioral outcomes after TBI

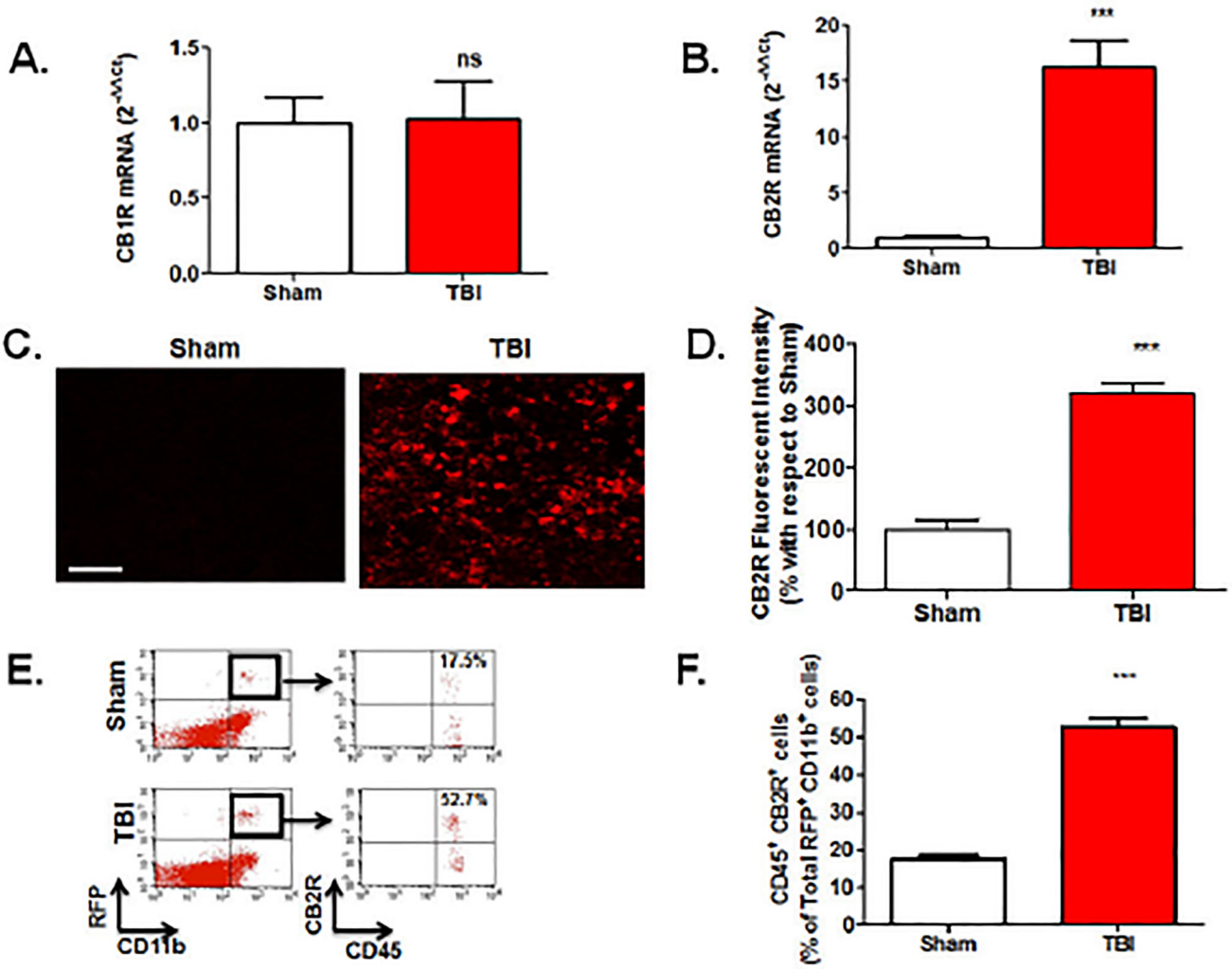

Fig. 1. Selective increase in CB2R expression after TBI

(A.) CB1R and (B.) CB2R mRNA were assessed in brain tissue by RT-qPCR and normalized to 18S expression. Data are expressed as fold change with respect to sham and revealed a selective 15-fold increase in CB2R expression. (C.) Histological analysis revealed increased $CB2R^+$ immunoreactivity in the injured cortex (Scale-50μm), as compared to sham-operated brains. (D.) $CB2R^+$ cells were quantified as mean fluorescent intensity and normalized to sham. (E.) Bone marrow chimera mice were generated whereby myeloid cells expressed red fluorescent protein (RFP). CB2R was expressed in 52.7% of $RFP^+CD11b^+CD45^{HI}$ infiltrating myeloid cells in the brain after TBI whereas 17.5% of RFP^+ cells expressed CB2R in sham brains, as assessed by flow cytometry. (F) Quantification of $RFP^+CD11b^+CD45^{HI}CB2R^+$ shown in panel (E.). Groups were compared as Student's t-test. Data were represented as mean ± SEM (n=6; **p<0.01; ***p<0.001 vs. sham).

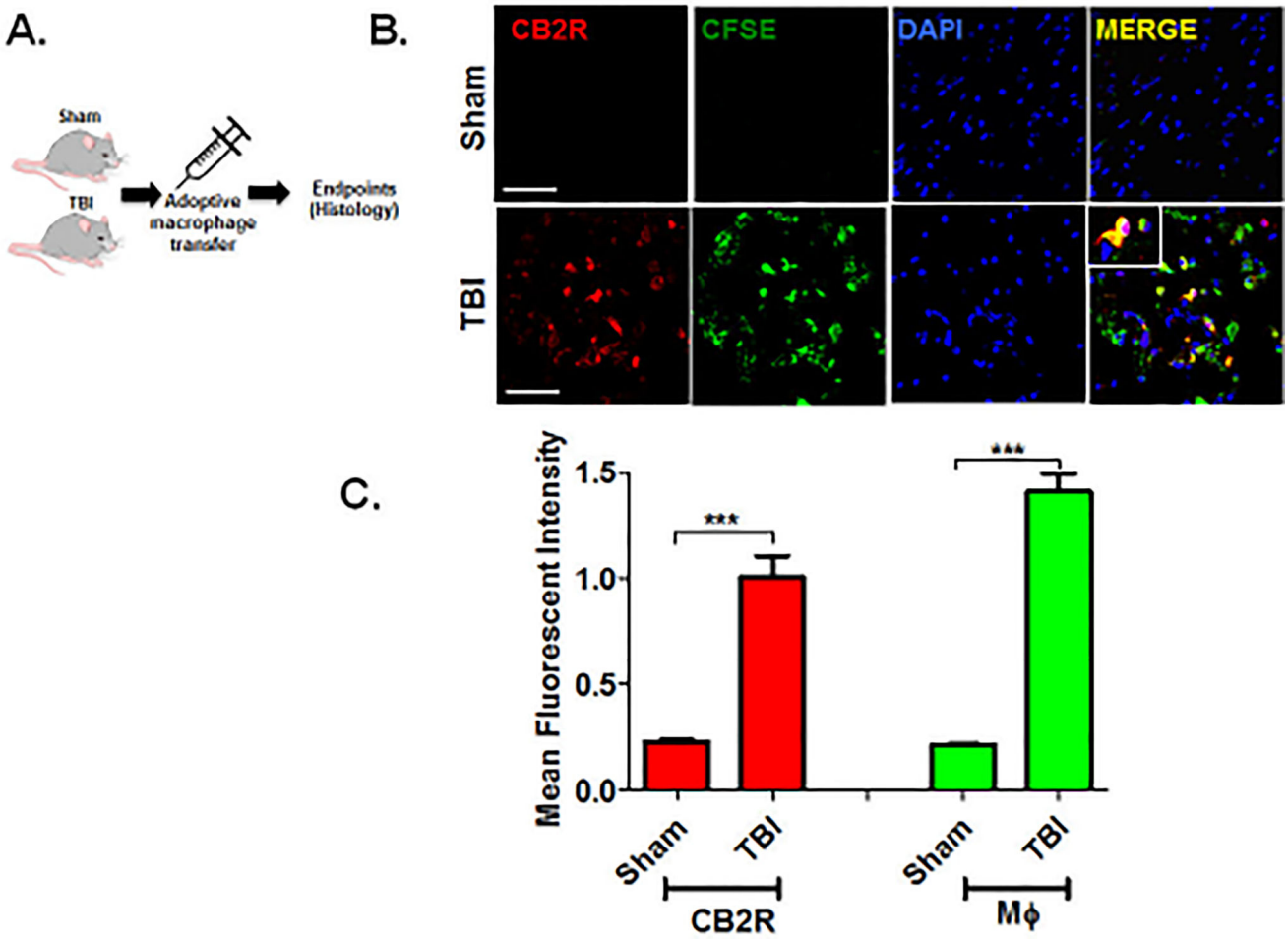

Fig. 2. CB2R expression in infiltrated myeloid cells after TBI

(A.) Schematic of macrophage (MΦ) adoptive transfer in recipient mice. CFSE-labeled $CD11b^+$, $CD68^+$, $F4/80^+$ macrophages were intravenously administered through the tail vein immediately after sham/TBI. Brains were harvested for immunofluorescent staining at 72h post-injury. (B.) The increased infiltration of $CFSE^+$ macrophages temporally and spatially paralleled increased $CB2R^+$ expression after TBI (Scale-50μm). (C.) $CB2R^+$ (red) and CFSE-labeled macrophages (green) were quantified as mean fluorescent intensity. Data were represented as mean ± SEM (n=6) and analyzed using Student's t-test (***$p<0.001$ vs. sham).

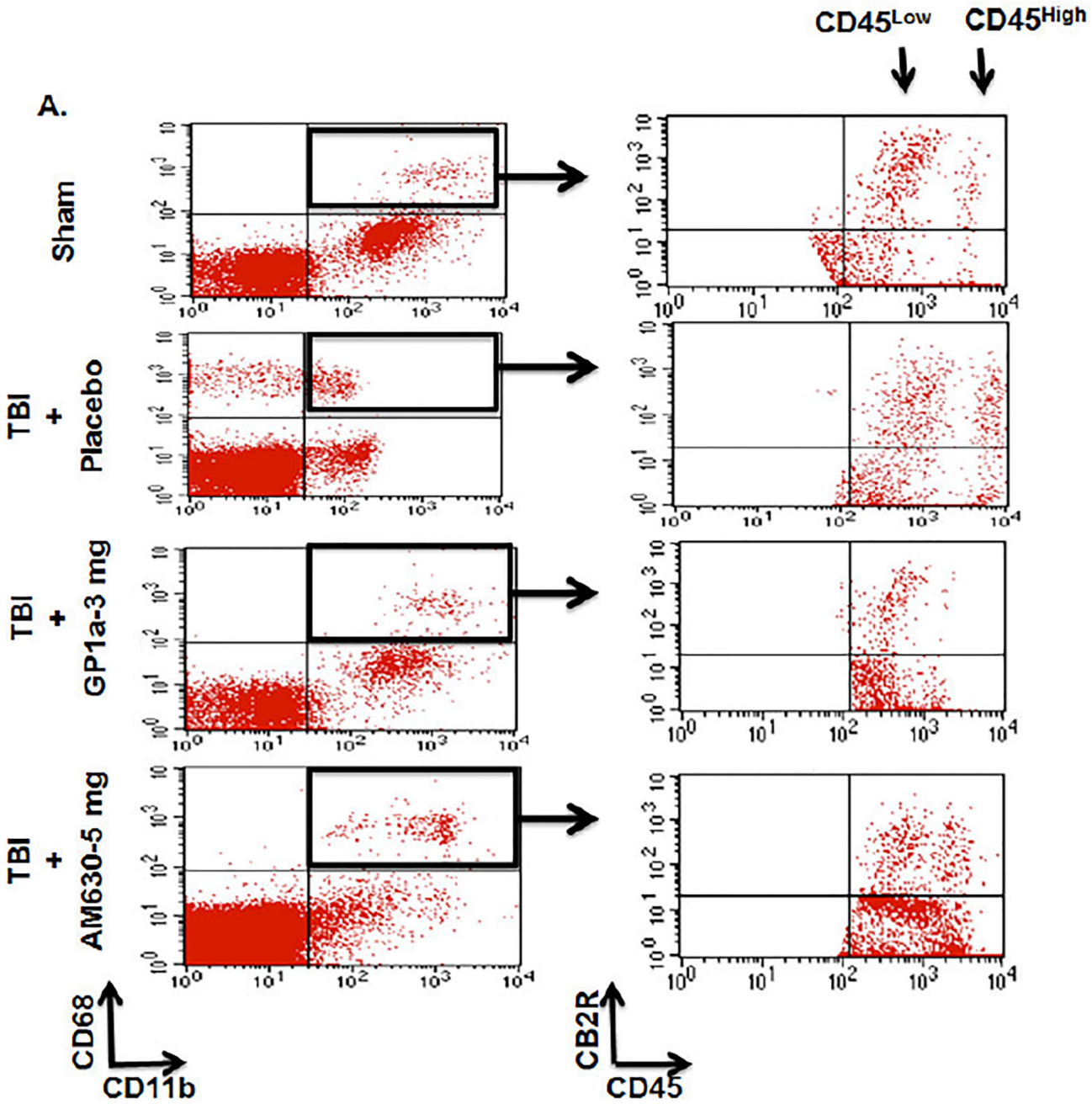

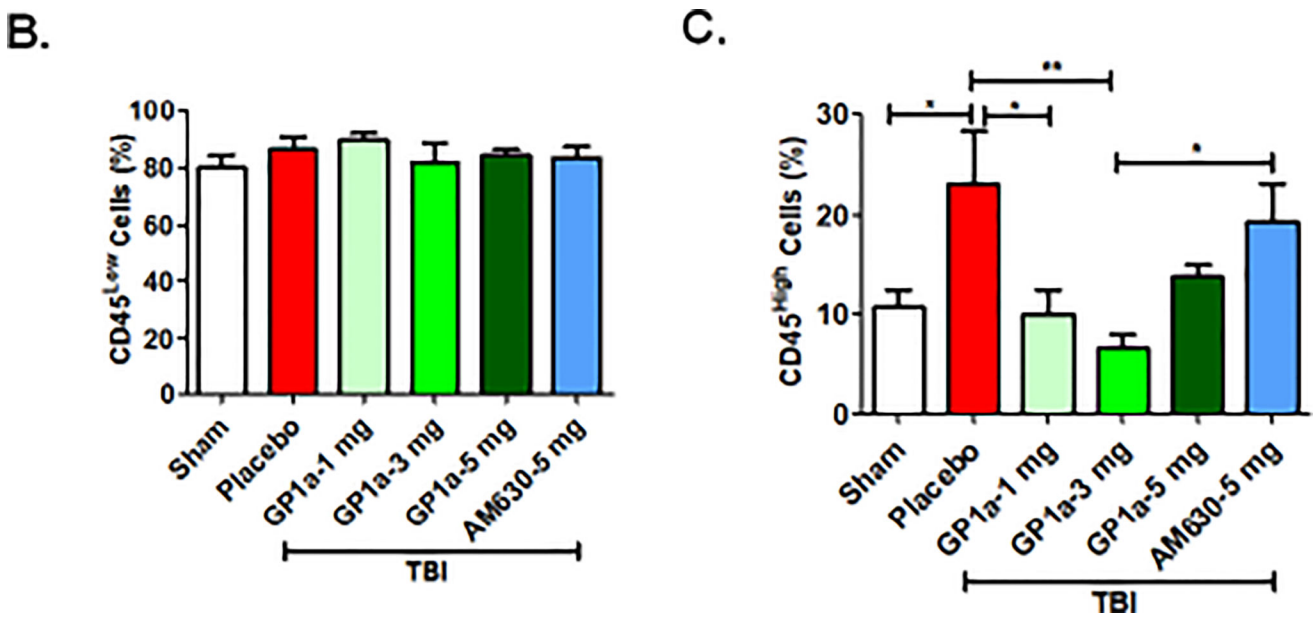

Fig. 3. CB2R activation decreases macrophage infiltration into the brain after TBI

(A.) Representative flow cytometry dot plots showing $CD68^{+}$ $CD11b^{+}$ $CB2R^{+}$ myeloid cells were sorted after sham/TBI and analyzed for microglia ($CD45^{Low}$) and infiltrating macrophages ($CD45^{High}$) populations. A TBI-induced increase in infiltrating macrophages was significantly reduced by treatment with GP1a (1 and 3 mg/kg), but not after treatment with the CB2R antagonist, AM360 (5 mg/kg). Interestingly, microglia did not show any significant alterations in numbers at day 3 post sham/TBI with or without treatment. Gating strategy has been shown in Fig 3A. Quantification of (B.) microglia and (C.) infiltrating macrophages are shown here. Data were represented as mean ± SEM and groups were compared by One-way ANOVA followed by Newman-Keuls multiple comparison. (n=6–7/group; *$p<0.05$; **$p<0.01$).

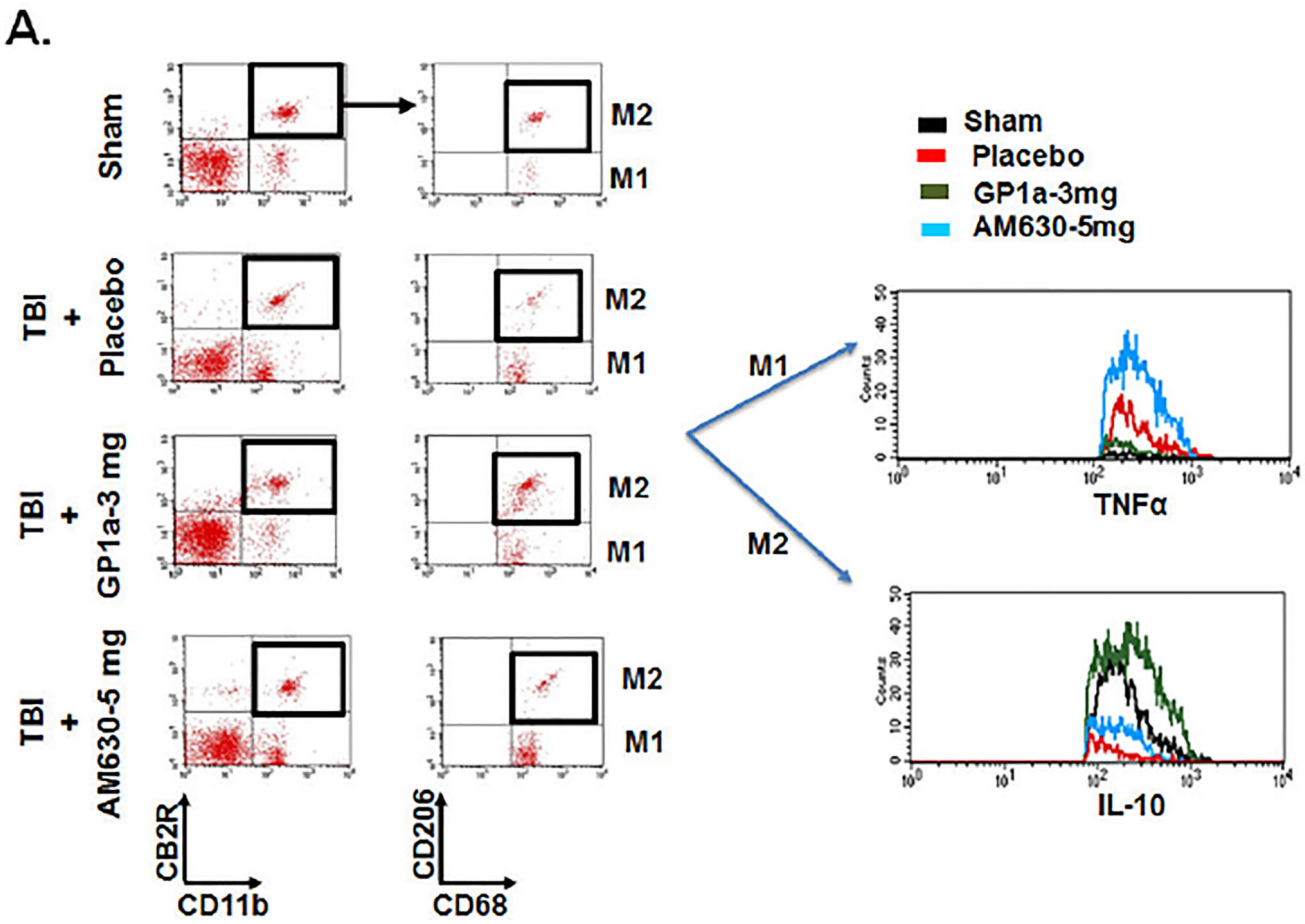

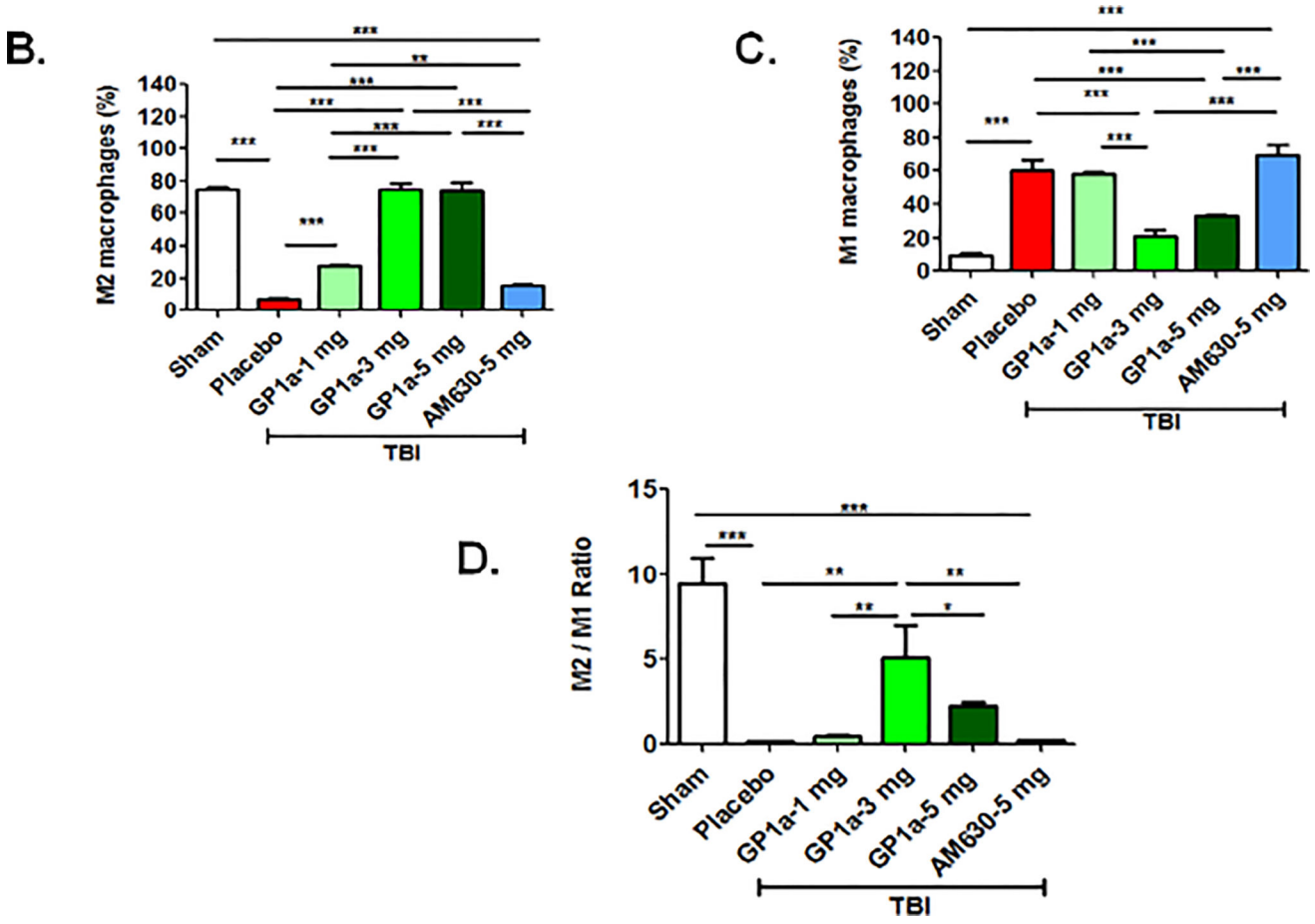

Fig. 4. CB2R activation increases M2 macrophage polarization after TBI

(A.) Representative flow cytometry dot plots showing $CB2R^+$ $CD11b^+$ myeloid cells were sorted after sham/TBI and analyzed for M1 ($CD68^+$ $CD206^-$ $TNF\alpha^+$) and M2 ($CD68^+$ $CD206^+$ $IL10^+$) polarization. A TBI-induced increase in M1 polarization was significantly reduced by treatment with 3 mg/kg GP1a, but not after treatment with the CB2R antagonist, AM360 (5 mg/kg). Dot plots for GP1a treatments (1 mg/kg b.wt and 5 mg/kg b.wt.) are not shown here. Quantification of (B.) M2 macrophages (C.) M1 macrophages, and (D.) the ratio of M2:M1 macrophages after treatment. Data were represented as mean ± SEM and groups were compared by One-way ANOVA followed by Newman-Keuls multiple comparison. (n=6/group; *p<0.05; **p<0.01; ***p<0.001).

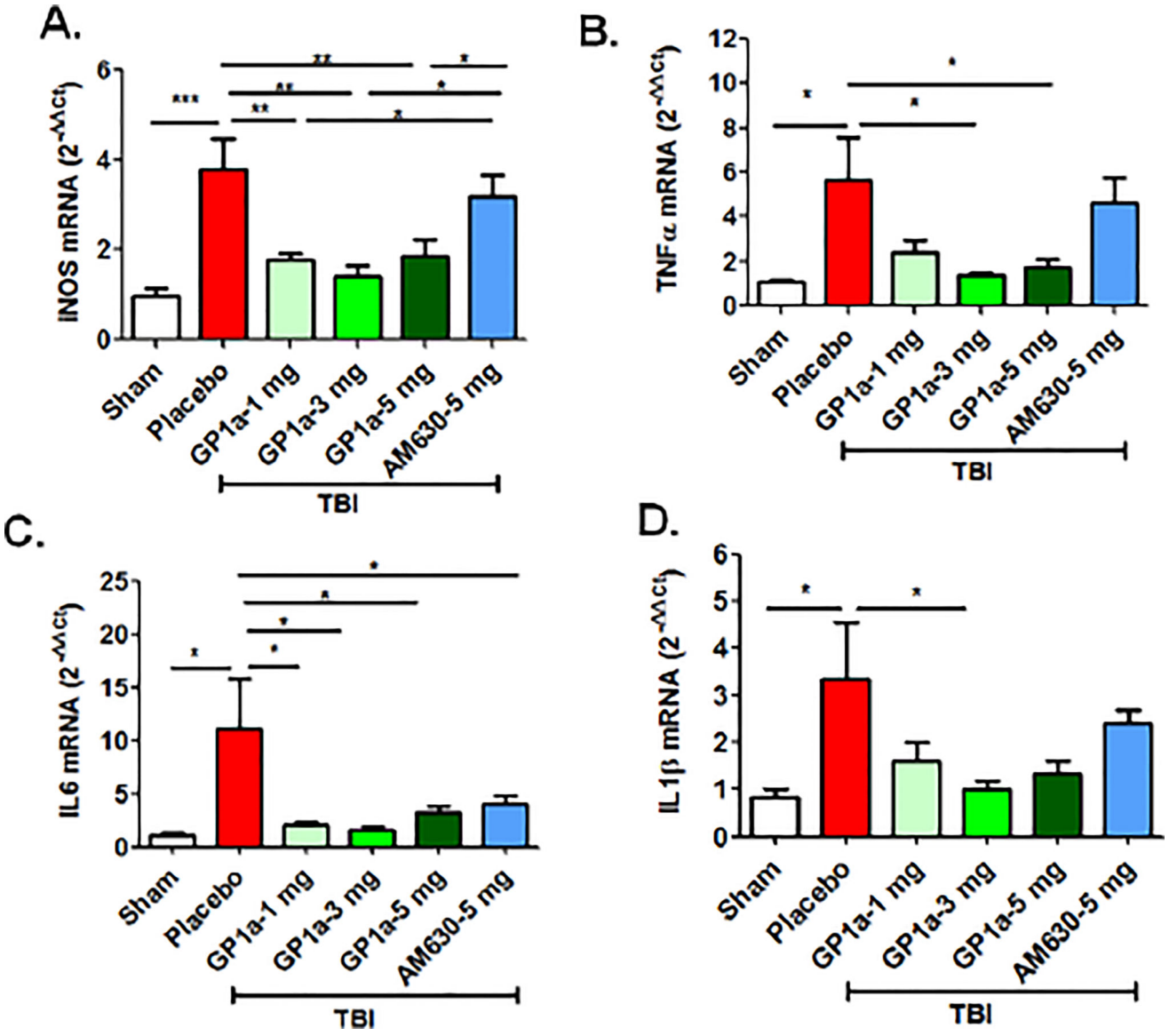

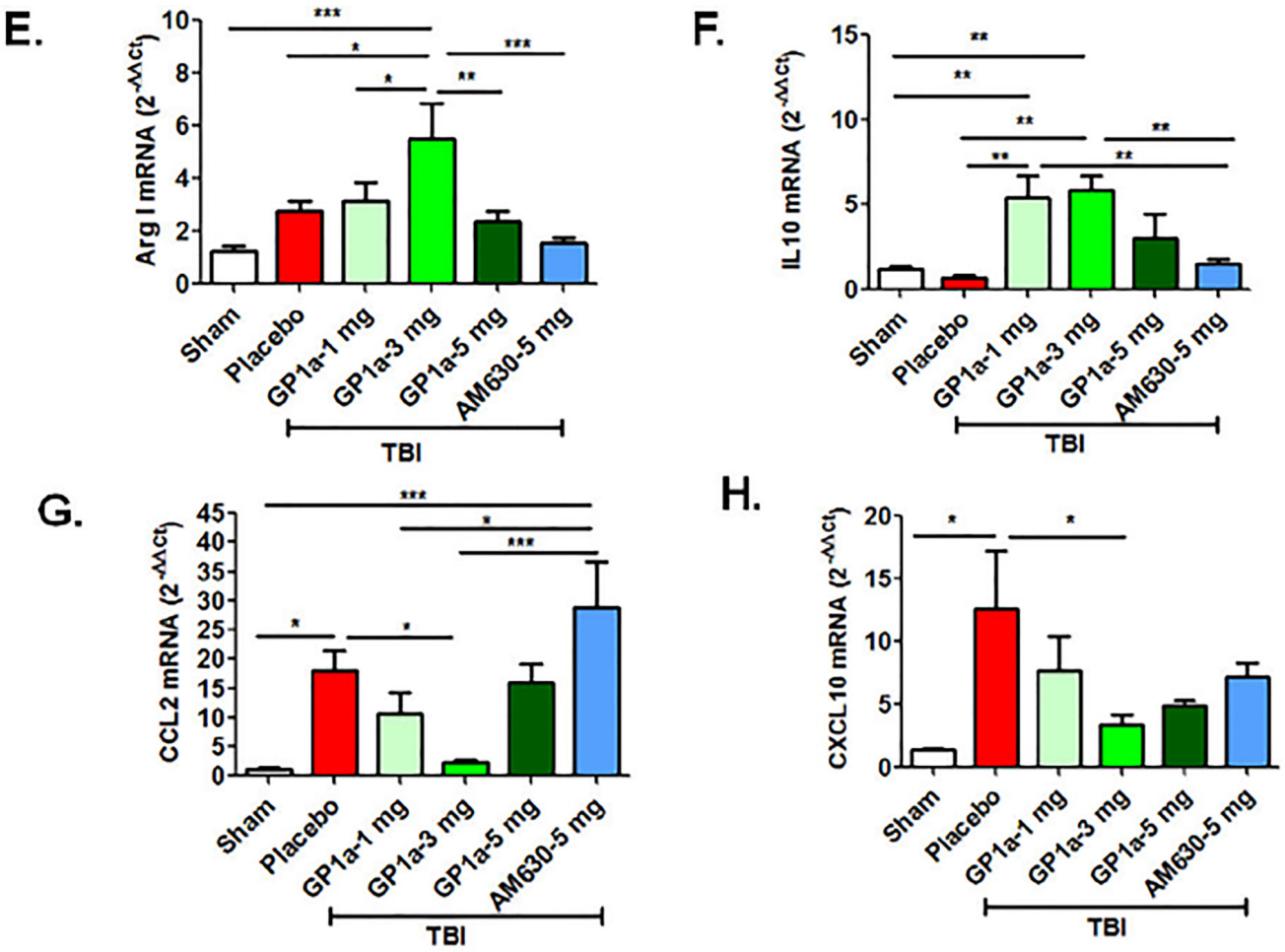

Fig. 5. CB2R activation reduces pro-inflammatory cytokine expression after TBI

Gene expression of inflammatory cytokines (TNF-α, IL-1β and IL-6), anti-inflammatory cytokine (IL-10), leukocyte chemo-attractants (CCL2 and CXCL10), and macrophage-associated enzymes (iNOS and Arg1) were quantified by qRT-PCR at 72h post-TBI. Treatment with GP1a reversed the TBI-induced expression of inflammatory mediators within the peri-contusional cortex whereas AM630 was largely ineffective, as compared to sham. Groups were represented as mean ± SEM (n=6/group) and analyzed using a One-way ANOVA followed by Newman-Keuls multiple comparison (*p<0.05; **p<0.01; ***p<0.001).

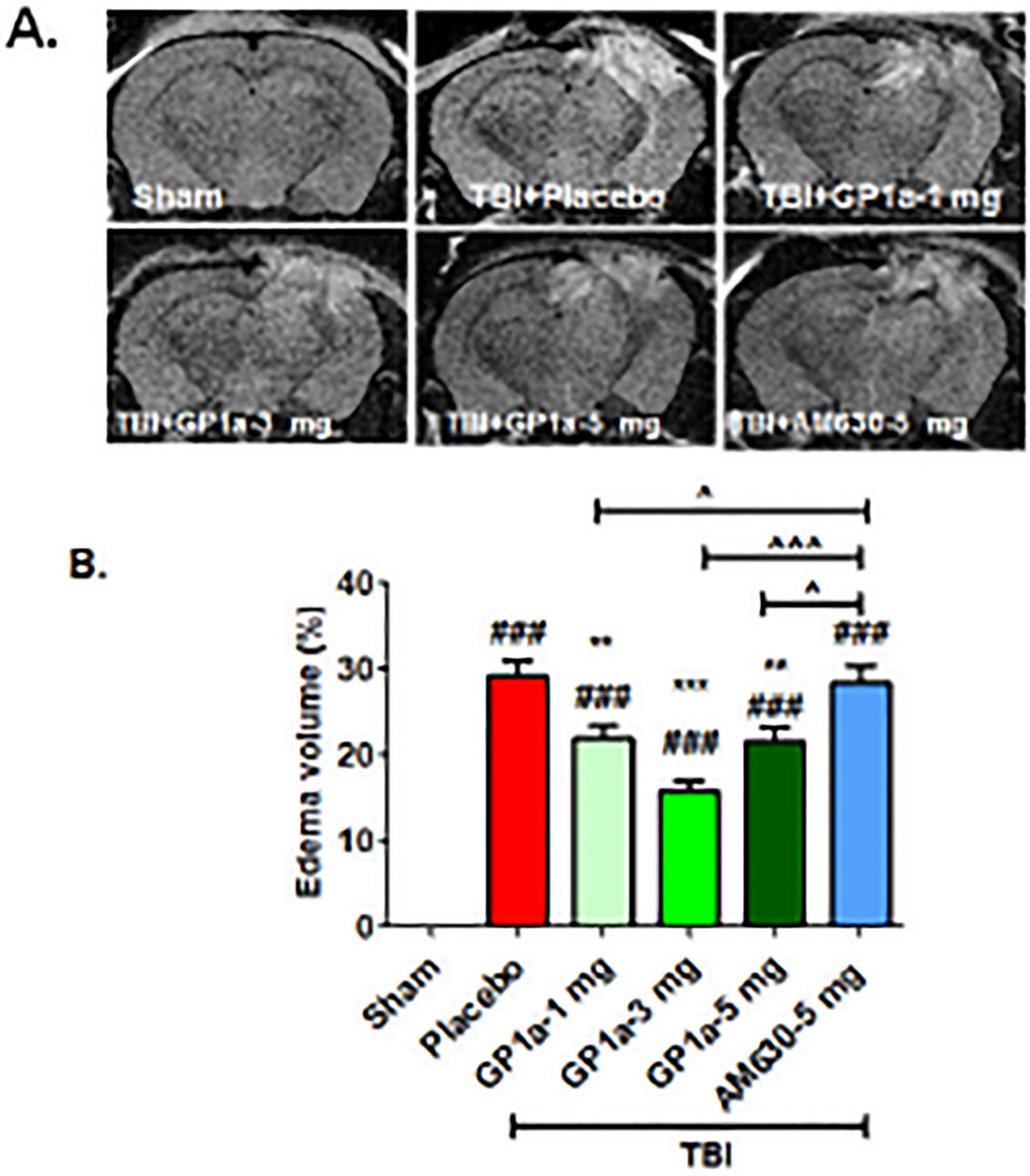

Fig. 6. GP1a reduced edema volume after TBI

(A.) Representative MRI images showing GP1a treatment reduced edema volume at 24h post-TBI. (B.) Data were quantified using ImageJ software and are expressed as mean ± SEM (n=6–8/group). Groups were compared using a One-way ANOVA followed by Newman-Keuls post-hoc test ($^{###}p<0.001$ vs. sham; **p<0.01; ***p<0.001 vs. placebo treated TBI; ^p<0.05; ^^^p<0.001 vs. 5 mg/kg AM630 treated mice after TBI).

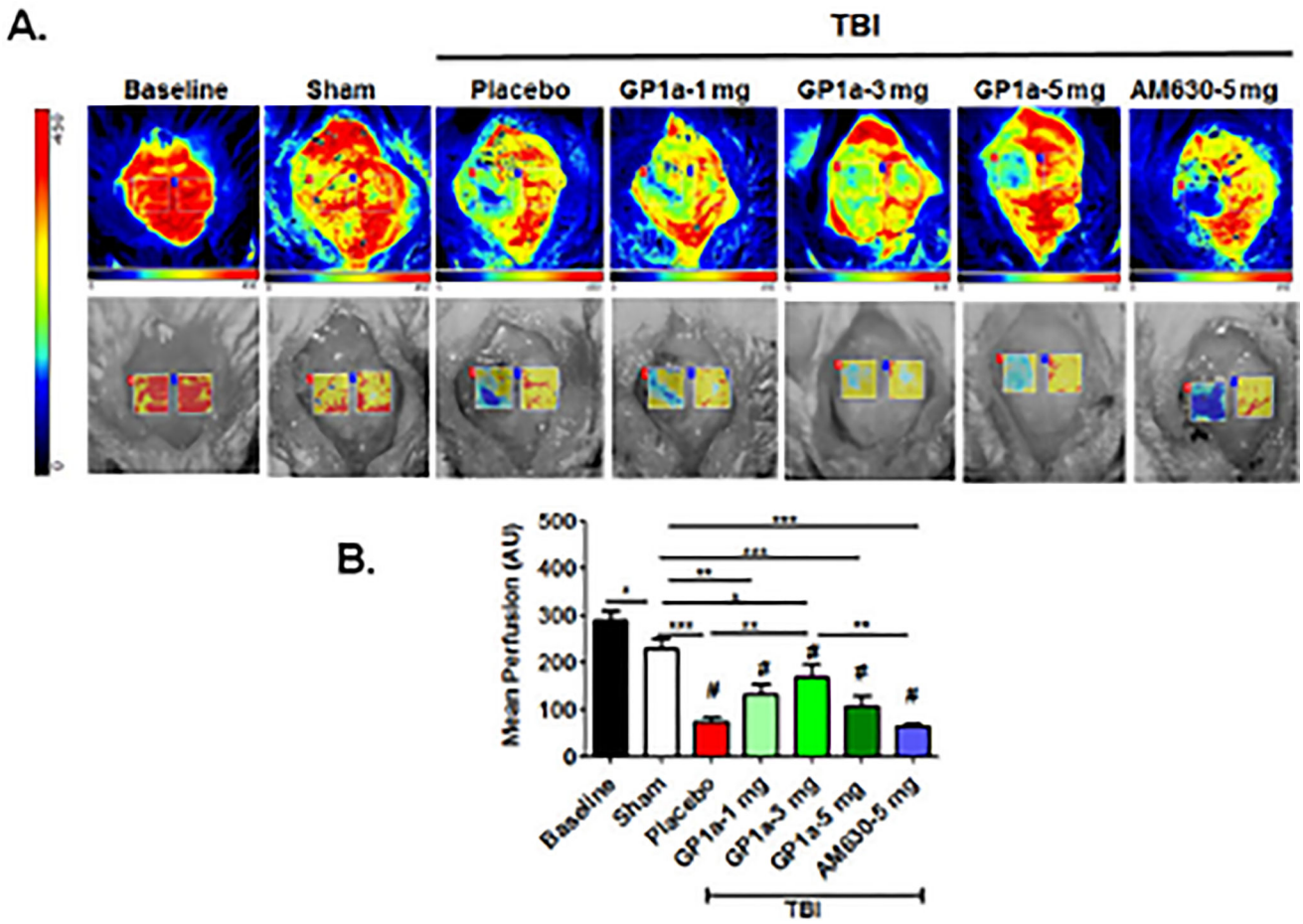

Fig. 7. GP1a improves CBF after TBI

A) CBF was imaged at baseline and at 24h post-TBI using LSCI. Representative images are provided following GP1a (1–5 mg/kg) or AM630 (5 mg/kg) treatment (B.) Cerebral perfusion was quantified as mean perfusion value and data were presented as mean ± SEM (n=6–7). Groups were compared as One-way ANOVA followed by Newman-Keuls multiple comparison (*p<0.05; **p<0.01; ***p<0.001 vs. placebo treated TBI; # p<0.05 vs. Sham).

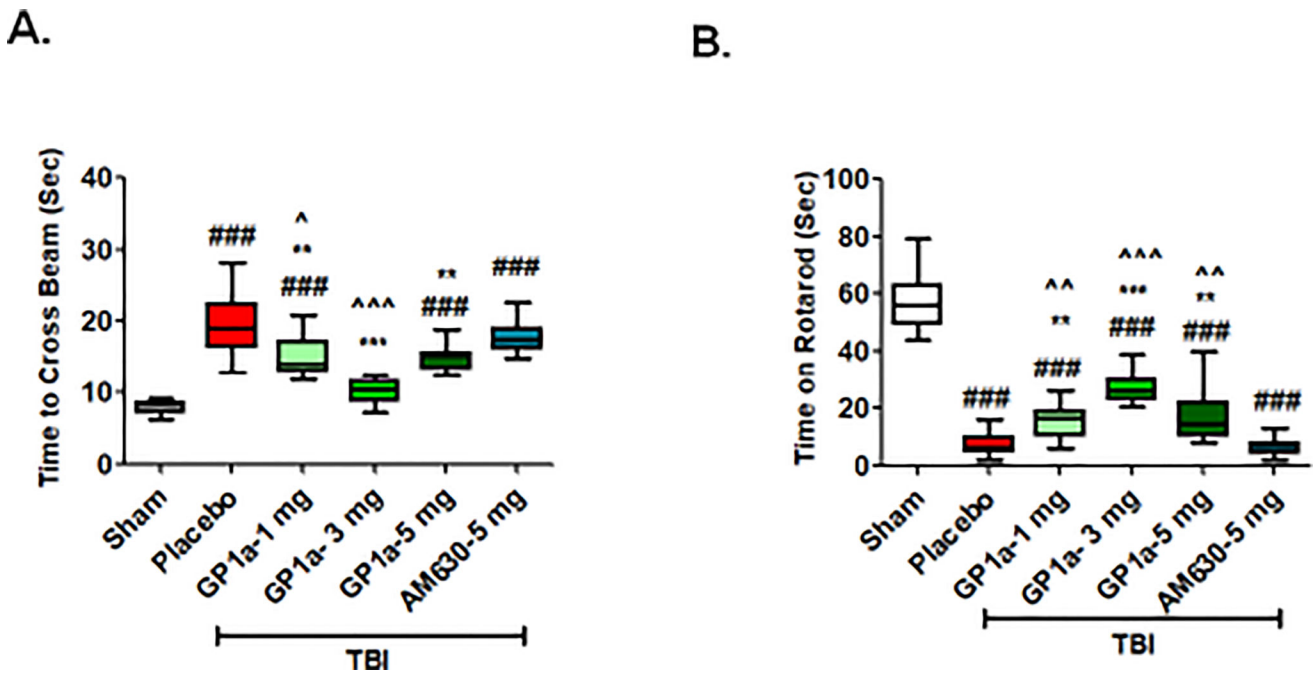

Fig. 8. GP1a improves motor function after TBI

Mice were tested on (A) stationary narrow beam and B) accelerating rota-rod for motor coordination. Placebo-treated TBI mice showed significant motor impairments on both tasks whereas all doses of GP1a improved outcomes. Data were represented as mean ± SEM (n=12). Groups were compared as One-way ANOVA followed by Newman-Keuls post hoc test ($^{###}p<0.001$ vs. sham; $^{**}p<0.01$; $^{***}p<0.001$ vs. placebo treated TBI; $^{\wedge}p<0.05$; $^{\wedge\wedge}p<0.01$; $^{\wedge\wedge\wedge}p<0.001$ vs. 5 mg/kg AM630 treated mice after TBI).

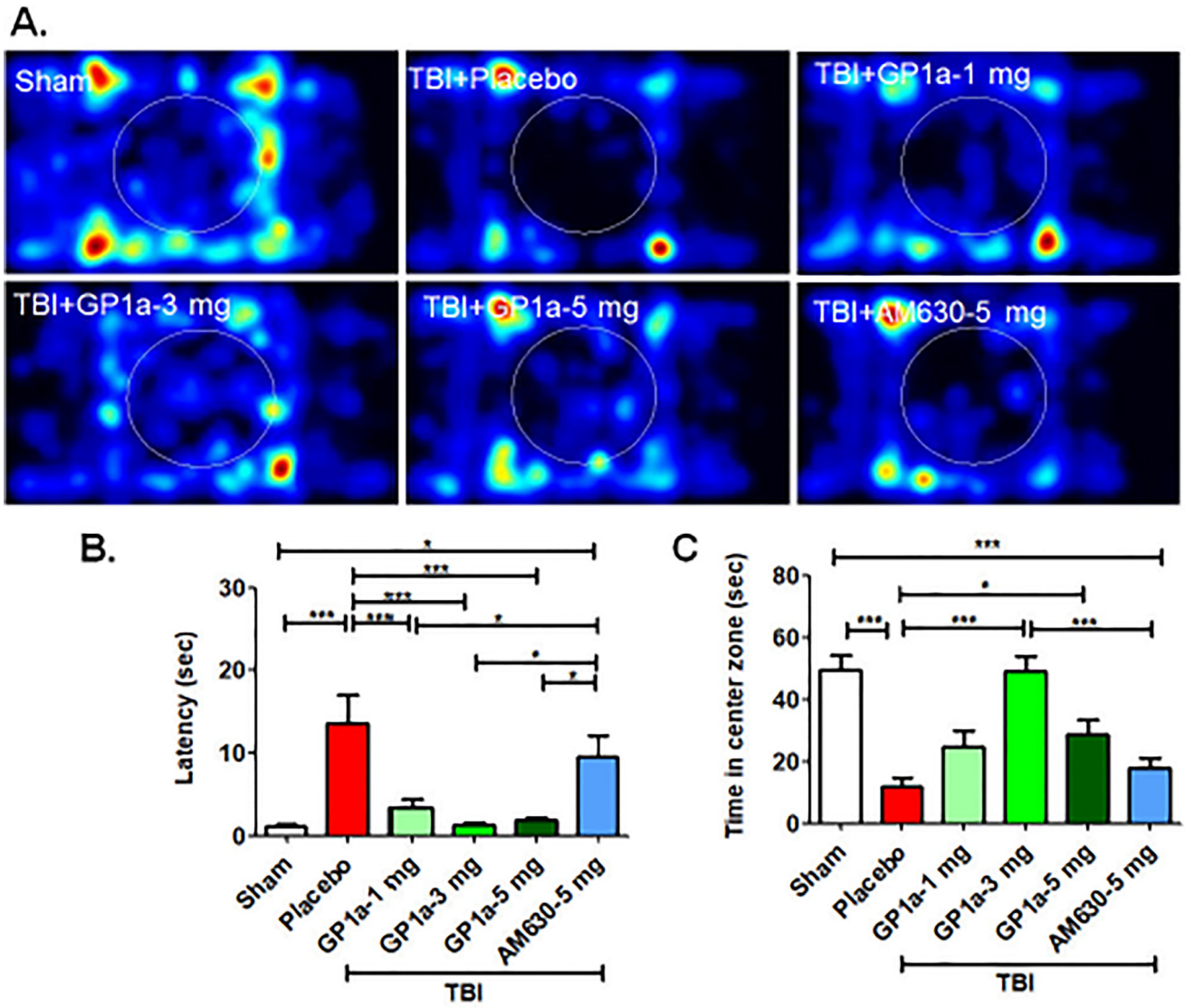

Fig. 9. GP1a exhibits anxiolytic effects after TBI

(A.) Representative heat maps from the open field task showed that GP1a (1–5 mg/kg) increased overall movement throughout the trial. (B.) Quantification of open field data showed GP1a (1–5 mg/kg), but not AM630, reduced the latency to enter center zone, a measure of reduced anxiety, and (C.) increased the time spent in the center zone. Data were expressed as mean ± SEM (n=12/group). Groups were compared by One-way ANOVA followed by Newman-Keuls post hoc test (*p<0.05 and ***p<0.001).

Table 1

Primers used for quantification of mRNA expression in brain by RT-qPCR.

Name	Sequence (5'-3')	Accession Number/Reference
Mm 18S rRNA - FP	GTAACCCGTTGAACCCCATT	NR_003278.3 (Schmittgen and Zakrajsek, 2000)
Mm 18S rRNA - RP	CCATCCAATCGGTAGTAGCG	
Mm Arg I - FP	CTCCAAGCCAAAGTCCTTAGAG	NM_007482.3
Mm Arg I - RP	AGGAGCTGTCATTAGGGACATC	
Mm IL10 - FP	TAACTGCACCCACTTCCCAG	NM_010548.2
Mm IL10 - RP	AGGCTTGGCAACCCAAGTAA	
Mm TNFα - FP	CCCTCACACTCAGATCATCTTCT	NM_013693.3
Mm TNFα - RP	GTCACGACGTGGGCTACAG	
Mm IL6 - FP	TAGTCCTTCCTACCCCAATTTCC	NM_031168.2
Mm IL6 - RP	TTGGTCCTTAGCCACTCCTTC	
Mm IL1β - FP	TGCCACCTTTTGACAGTGATG	NM_008361.4
Mm IL1β - RP	AAGGTCCACGGGAAAGACAC	
Mm iNOS - FP	GTTCTCAGCCCAACAATACAAGA	NM_010927.4
Mm iNOS - RP	GTGGACGGGTCGATGTCAC	
Mm CXCL10 - FP	AAGTGCTGCCGTCATTTTCT	NM_021274.2
Mm CXCL10 - RP	GTGGCAATGATCTCAACACG	
Mm CCL2 - FP	CCACAACCACCTCAAGCACT	NM_011333.3
Mm CCL2 - RP	TAAGGCATCACAGTCCGAGTC	
Mm CB1R - FP	AAGTCGATCTTAGACGGCCTT	NM_007726.3
Mm CB1R - RP	TCCTAATTTGGATGCCATGTCTC	
Mm CB2R - FP	CTACAAAGCTCTAGTCACCCGT	NM_001305278.1
Mm CB2R - RP	CCATGAGCGGCAGGTAAGAAA	

[#]Mm – *Mus musculus*; FP - Forward Primer; RP- Reverse Primer